Chapter 1 Introduction

1.1 Background

The design and construction of AC machines is quite simple and it's an electromechanical energy conversion. Generally, majority of the induction machines (IM) are squirrel-cage rotor type because of many advantages i.e. rotor is inaccessible; there is no moving contact, such as commutators and brushes unlike in dc machines where the risk is more. An IM not only reduces the risk of sparking, but also reduces the atmospheric explosion. There is no wiring in the rotor windings which increases the ruggedness of the machines. These machines can run at high speeds and withstand heavy electrical and mechanical loads. In adjustable-speed drives (ASDs), the low electric time constant speeds up the dynamic response to control commands (Trzynadlowski, 2001).

The study of IM can be explained in two ways either by evaluation of design or by analysis of machine operation. The first method is based on empirical rules which make us to think about various questions such as what is the dimension, how to construct so on and so forth. Where as the second one is based on function and control of IM i.e. mathematical tools, variables and parameters are largely used. Although our project is emphasises mainly on second aspect i.e. the equivalent circuits of IM which consists of stator and rotor resistance, R_1 and R_2, stator and rotor phase leakage inductance L_1 and L_2, and the principal of inductance of the stator phases L_p An as an auxiliary parameter related to the principal inductance, namely the magnetising inductance, L_o (Amin, 2002).

In general, IMs are significant to torque reserve characteristics. The rarely used wound-rotor induction motors are used in some special cases, the impact of accessibility of the rotor winding is an advantage. The winding can be reached via brushes on the stator that ride atop slip rings on the rotor. The motor current can be reduced by adjusting resistors which are connected to the winding during start-up of the drive system. As soon as the motor reached the operating speed windings, the terminals are short circuited. Wound rotor motors are cascaded which draws an

excess power to control the speed unlike in squirrel-cage induction motor. The operating principles of induction motors remain unchanged. From the past three decades, the research on the motors has been significantly changed i.e. motors were designed smaller, lighter, more reliable and efficient. This motor is so-called *high-efficiency motors***,** which are quite expensive, when compared to other motors. Practically, the average life span of an induction motor can be assumed to be about 12 years (Trzynadlowski, 2001).

Nowadays, AC machines are easily available in the market. AC machines plays an important role in the industry for instance, large size AC motors drive pumps and cranes in production plants where as small size AC motors are used in domestic purposes such as fans, clocks so on. Generally AC motors are available in different sizes and shapes which is designed to use both single and three phase power (Humphries, 1998).

1.2 Electric Energy of an Induction Machine (IM)

(Mendrela et al., 2003) Induction motors are commonly applied to machines in electric drive systems. Consider, a squirrel cage induction motor (Boldea, 2001) these motors have been traditionally fed directly from the three phase AC electric power grid through electromagnetic power switches with adequate protection. (Boldea, 2001) Today in developed countries there are more than 3 kW of electric motors per person are induction motors. And 10% of all induction motor power is converted into variable speed drives which have been 9% in the last decade while the electric motor markets showed an average annual growth rate of 4% in the same time. Variable speed drives with induction motors are used in pumps, machine tools, robotics, washing machines etc.

The prediction for the future is such that 50% of all the electric motors will be fed through power electronics with induction motors covering 60 to 70% of these new markets (Mendrela et al., 2003). However, there is a large group of linear motors available in the market; rotating motors are predominant among IMs. After 1885, the impact of the induction motor came like juggernaut, presently in all industries and in home applications; the IM is ready to make the electric starter/generator system

aboard the hybrid vehicles of the near future. The important points to be considered in modelling and optimization design in the era of finite element methods are its control as a motor and generator for even better performance when supplied from PWM converters (Mendrela et al., 2003).

1.3 Overview of the thesis

The objective of this dissertation is to estimate rotor flux of an IM. Some of the material is focused on the functional block of the IM i.e. Torque estimator, Speed estimator etc. while a subsequent part deals with estimation of rotor flux. The dissertation is organized as follows:

Chapter 1 describes background information of the machines then it focuses on the methodology how on to approach the task on a particular time with the help of Gantt chart.

Chapter 2 presents the basic principals of rotating magnetic field of the IM and asserts brief overview of the AC machines. Later it talks about different kinds of IM rotors suggesting which one is good. It is crucial to start with good and appropriate reviews which were verified by numerous journals. Literature review is presented by analysing the previous work. (Busawan et al., 2001) summarises that a nonlinear observers for the estimation of the rotor flux and the load torque in an induction motor. The observers are designed on the basis of the standard α - β *Park's model.* Finally, fuzzy logic is mentioned in more detailed way and Membership functions were also discussed

Chapter 3 explains the dynamic model of induction machine plant and the model was presented. Then the model is analysed, developed in MATLAB-SIMULINK which was discussed in Chapter 4. By considering following assumptions, dynamic model is implemented i.e. it should be symmetrical two-pole, three phase windings. Slotting effects are neglected, Permeability of the iron part is infinite, and iron losses are neglected. Dynamic d-q model and Axes transformation is implemented on stationary reference frame (a-b-c). Lastly torque equation is derived.

Chapter 4 is the heart of this project by scrutinizing the model thoroughly and by introducing fuzzy controller logic using MATLAB-SIMULINK; simulations are performed to estimate the functional block such as torque, speed, flux, resistance with and without fuzzy logic. Results were obtained for different blocks and the m-file, DTC, Flux table were obtained and presented in the Appendixes.

Chapter 5 concludes the simulation results and concentrates mainly on the future direction what more can be done to improve the platform in a more efficient manner.

1.4 Methodology

The methodology is focussed on the steps to achieve the research objective i.e. the aim of this project is to design a non-linear observer for the estimation of rotor flux variables that are normally not measurable in an induction motor system.

Step1 Familiarity with the standard mathematical model of induction motors.

Step2 Study of a newly developed non-linear observer design technique.

Step3 Design of an observer for the rotor flux estimation.

Step4 Setting-up of MATLAB-SIMULINK simulation platform.

Step5 Simulation and analysis of the designed rotor flux estimator.

Chapter 2 Rotating magnetic field

Rotating magnetic field is defined as a field which changes its direction at a constant angular rate. All the AC current motors work on this principle. In general, both AC and DC motors produces Torque by the interaction of stator and rotor separated by a small air gap. For a wound-field DC motor the current flows in only one direction through the rotor windings which in turn produces torque unlike in Synchronous and induction motor (Humphries, 1998).

The basic principle to understand the concept of rotating field is shown in figure 2.1.Consider two permanent magnets; one is placed at the middle named as permanent-magnet rotor and the other magnet which rotates around the rotor electronically. The influential of the field in turn pulls the rotor magnet in the same direction. In general, any motor has two elements i.e. one rotating part called the *Rotor* and stationary part called *Stator*. Even though stator is not made to rotate physically but it could be made to rotate magnetically. This phenomenon is termed as Rotating magnetic field (Humphries, 1998). The number of pole pairs should be similar with phases in the applied voltage and also stator poles must also be physically displayed from each other by an angle equal to the phase angle between the individual phases of the applied voltage (Humphries, 1998).

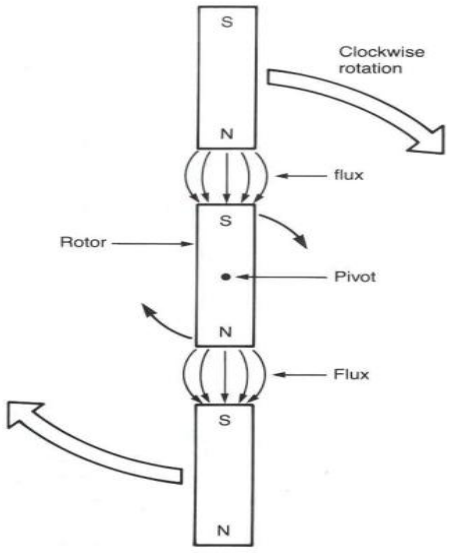

Figure 2.1 two rotating fields (Humphries, 1998)

(Humphries, 1998) The voltages applied to phase AA' and BB' are 90° out of phase, the current flow in AA' and BB' are 90° out of phase. The magnetic fields created in the coils are in phase with the currents, the magnetic fields are also 90° out of phase with each other. The combination of two out-of-phase magnetic fields forms a single total field. For every AC cycle this total field rotates one complete revolution (Humphries, 1998). The current has a phase difference of 90°. For this case if the current is negative, it states that current is flowing in one direction but when the current is positive, direction of the flow is in opposite direction.

Case 1

I_0 is zero at time t_0 in the AA' winding where as current I_0 is maximum in the BB' winding. From the Fleming's left-hand thumb rule we can state the position of the stator which is in north-south field as shown in figure 2.2 (a) (Humphries, 1998).

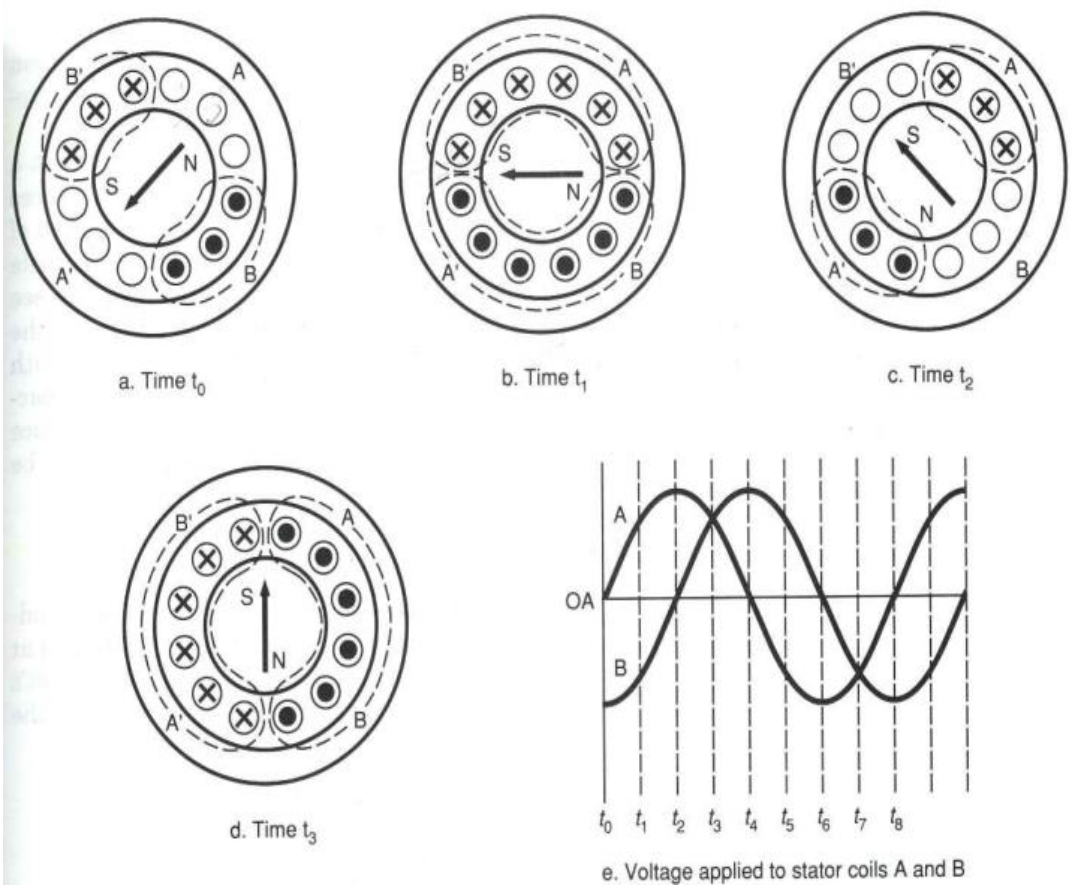

Figure 2.2 Two-Phase rotating fields (Humphries, 1998)

Case 2

At time t_1, I_B has decreased but I_A is positive at this instant both amplitudes are similar. The current in the winding BB' has decreased, but the field is in the same direction. As shown in figure 2.2 (b) the flux due to AA' and BB' are right angles to each other. North Pole of the resultant field has moved to 45° clock wise direction (Humphries, 1998).

Case 3

At time t_2, I_A is maximum and I_B is zero. The maximum current is flowing in AA' winding and there is no flow in BB' and the resultant field is shown in the figure 2.2 (c) Each time the phase of the currents leads 45°electrical, the resultant magnetic field rotates 45° mechanical (Humphries, 1998).

Case 4

At time t_3, both currents are positive and equal in amplitude. The direction of the currents in windings BB' is the reverse of that in figure 2.2 (a) and (b). The magnetic fields caused by the currents in two windings combine to form a vertical resultant field, as shown in figure 2.2 (d). If we continue this process from t_4 to t_8 the field continues to move in a clock wise direction as soon as the resultant field back in it is original positions as shown in figure 2.2 (a). For every single cycle of AC, the resultant field has rotated one complete revolution. The speed of the rotating field is equal to the supply frequency (Hertz) (Humphries, 1998).

Low-power FHP machines are available in single-phase, but poly-phase (three-phase) machines are used more often in variable-speed drives (Bose, 2002). Figure 2.3 shows an idealized three-phase, two-pole induction motor where each phase winding in the stator and rotor is represented by concentrated coil. The three-phase windings, connected in *wye* or *delta* form, are distributed sinusoidally and embedded in slots. In a wound-rotor machine, the rotor winding is similar to that of the stator but in a cage machine, the rotor has a squirrel cage-like structure with shorted end rings. Basically, the machine can be looked upon as a three-phase transformer with a rotating and short-circuited secondary. Both stator and rotor cores are made with

laminated ferromagnetic steel sheets. The air gap in the machine is practically uniform (non-salient pole) (Bose, 2002).

A sinosoidally balanced power supply in three-phase stator winding creates a synchronously rotating magnetic field (Bose, 2002).

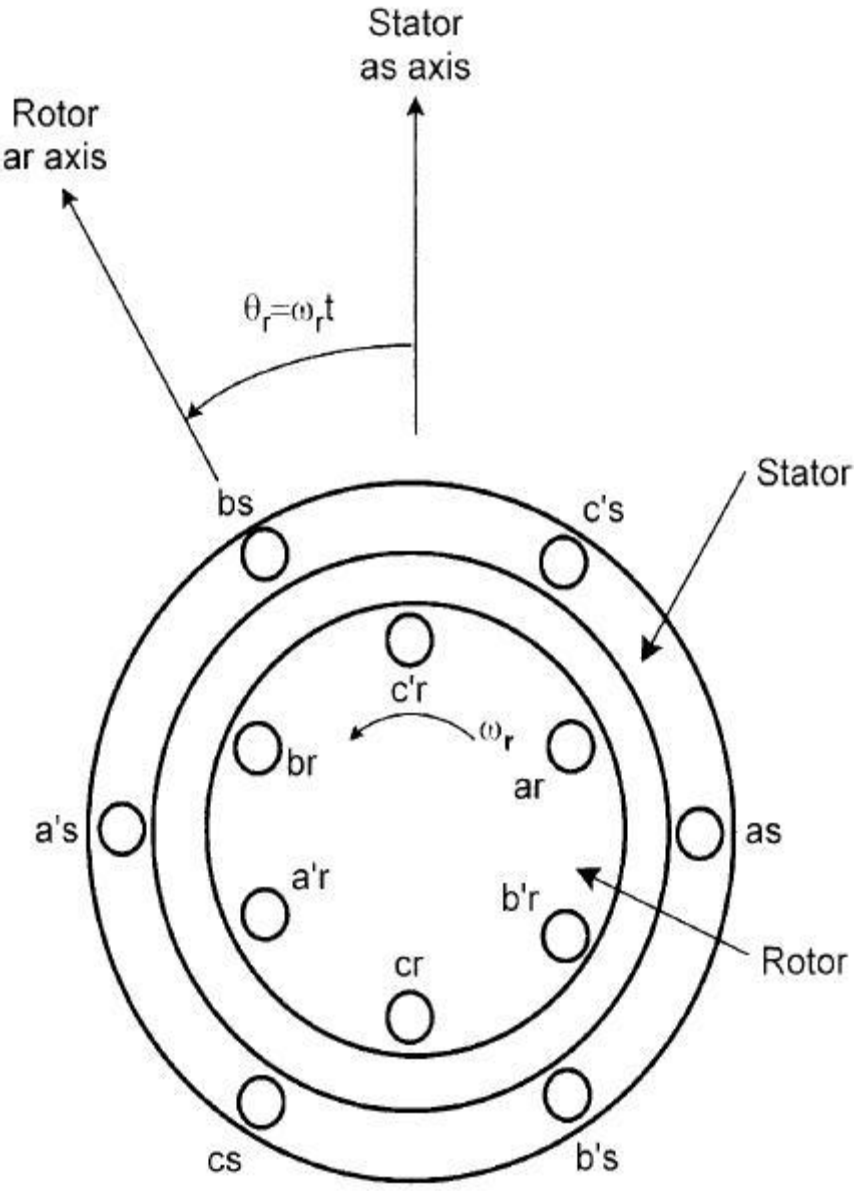

Figure 2.3 Idealized three-phase, two-pole induction motor (Bose, 2002)

Consider that three-phase sinusoidal currents are impressed in the three-phase stator windings,
as shown in figure 2.4.

$$i_a = I_m \cos \omega_e t \tag{1.1}$$

$$i_b = I_m \cos\left(\omega_e t - \frac{2\pi}{3}\right) \tag{1.2}$$

$$i_e = I_m \cos\left(\omega_e t + \frac{2\pi}{3}\right) \tag{1.3}$$

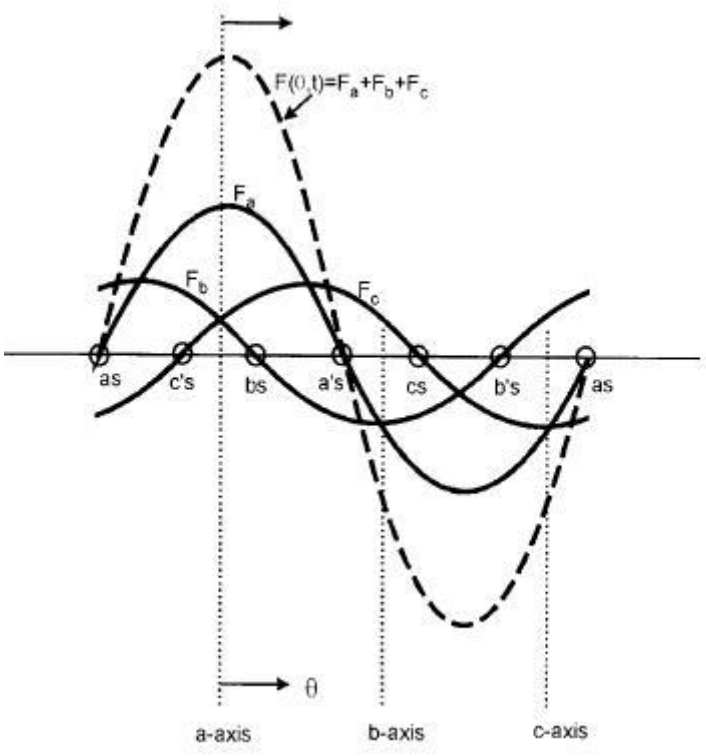

Figure 2.4 MMF distribution in three winding of stator (Bose, 2002)

Each phase winding will independently produce a sinusoidally distributed mageneto-motive force (mmf) wave, which revolves around it's own axes. Figure 2.4 shows the mmf waves at time t=0 when $i_a = I_m$, $i_b = -I_m/2$ $i_e = -I_m/2$

At spatial angle θ, the instantaneous MMF expressions can be given as

$$F_a(\theta) = Ni_a \cos\theta \tag{1.4}$$

$$F_b(\theta) = Ni_b \cos\left(\theta - \frac{2\pi}{3}\right) \tag{1.5}$$

$$F_c(\theta) = Ni_c \cos\left(\theta + \frac{2\pi}{3}\right) \tag{1.6}$$

Where

N = Number of turns in a phase windings.

Magneto motive force (MMF) waves are phase-shifted in space by 2π/3 angle.

$$F(\theta) = F_a(\theta) + F_b(\theta) + F_c(\theta) = Ni_a \cos(\theta) + Ni_b \cos\left(\theta - \frac{2\pi}{3}\right) + Ni_c \cos\left(\theta + \frac{2\pi}{3}\right) \quad (1.7)$$

Substituting Equations (1.1) through (1.3) in (1.7) gives

$$F(\theta,t) = NI_m[\cos\omega_e t\cos\theta + \cos\left(\omega_e t - \frac{2\pi}{3}\right)\cos\left(\theta - \frac{2\pi}{3}\right) + \cos\left(\omega_e t + \frac{2\pi}{3}\right)\cos\left(\theta + \frac{2\pi}{3}\right)] \quad (1.8)$$

Simplifying Equation (1.8), the $F(\theta,t)$ expression can be written as

$$F(\theta,t) = \frac{3}{2}NI_m\cos(\omega_e t - \theta) \quad (1.9)$$

Equation (1.9) indicates that a sinusoidally distributed MMF wave of peak value $\frac{3}{2}NI_m$ rotating in air gap at synchronous speed ω_e. In a two-pole machine, $F(\theta,t)$ makes one revolution per cycle of current variation. This means for a P-pole machine, the rotational speed can be given as (Bose, 2002).

$$N_e = 120\frac{f_e}{P} \quad (1.10)$$

Where

N_e = synchronous speed in rpm

And f_e = stator frequency in hertz (Hz)

2.1 AC Machines

AC motor is an Electric motor that is driven by an alternating current. AC motor is divided into two parts

a) Stator having coils supplied with AC to produce a rotating magnetic field.

b) Rotor attached to the output shaft that is given a torque by the rotating field.

The magnetic field on the rotor is created either by permanent magnet or current delivered through slip rings. On the other hand, magnetic field on the rotor is created by induced current.

The Electrical machine which converts electrical energy to mechanical energy, is the workhorse in a drive system. Electric drive systems are widely used in applications such as pumps, fans, paper and textile mills, home appliances, wind generation systems, etc. Even though the principal of IMs were discussed long back ago by gullible people, still people are finding the better ways to estimate or implement the design of the IMs it is something like drop in the ocean. To design a high-performance drive system following points has to be kept in mind i.e. machine performance, dynamic model, and parameter variations. Industrial drive applications are generally classified into constant-speed and variable-speed drives. AC machines with a constant frequency sinusoidal power supply have been used in constant-speed applications, where as dc machines prefer Variable-speed drives. Commutators and brushes, in addition, limit the machine speed and peak current, cause EMI (Electromagnetic Induction) problems, and do not permit a machine to operate in dirty and explosive environments. Although dc machine drive converters and controls are simple, torque response is very fast (Bose, 2002).

AC machines are generally classified as follows

1) Induction Machines
   Cage or wound rotor (doubly-fed)
   Rotating or linear
2) Synchronous machines
   Rotating or linear
   Reluctance
   Wound field or permanent magnet
   Radial or axial gap (disk)
   Surface magnet or interior (buried) magnet
   Sinusoidal or trapezoidal
3) Variable Reluctance machines
   Switched reluctance

Stepper

2.2 Induction Machines (IMs)

(Sakae, 1986)Induction Machine is widely used in domestic and industry purposes. IM rotor gets its power by Faradays law of electromagnetic induction; AC voltages are induced in the rotor by the rotating magnetic field in the stator Humphries (1998). The stator can be considered as the primary, while the rotor acts a rotating secondary. The production scale of induction is more compared to other motors. However, its applications are limited to those that do not require a high level of control of speed, torque so on. The induction motor is an AC motor fed by an AC power supply. AC power systems are widely used throughout the world and are essentially fixed-voltage, fixed-frequency system. The induction motor has remained essentially a constant-speed motor, and its control capabilities have been markedly inferior to those of the DC motor Sakae (1986). The induction motor has begun to replace dc motors as a spindle motor of the lather is going to replace dc motor in the steel industry, as drive motors in steel mills and conveyor rolls; and is being tried as a primary motor in railway locomotives and electric trains.

The performance of an induction motor is dependent on power supply and control method used. When the power supply is fixed Voltage, fixed frequency, its performance is rather *limited* and it is inferior in control performance to the dc motor. When the power supply is of variable frequency, variable voltage, its performance is enhanced and its control performance becomes superior (Sakae, 1986).

A machine with only amortisseur windings is called an IM because the rotor voltage (generates the rotor current, magnetic field) is induced in the rotor windings rather than being physically connected to wires. The important feature of an induction motor is that *no dc field current is required to run the machine***.** Induction machines can be used as both generators and motors but in most cases it's often called motor because induction generator has lot of drawbacks (Stephen, 2005).

2.3 Design Method of Operation

The rotor of IM is connected in two ways

(a) Slip ring rotor

(b) Squirrel-cage rotor

2.3 (a) Slip ring rotor

IMs with slip-ring rotor consist of three-phase windings similar to stator with a number of phases m_2=3. Terminal windings are outside the cylindrical cage connected to slip rings. Where as rotor windings are short-circuited by two ways either directly or via brushes using a starting resistor or can be supplied by external voltage.

2.3 (b) Squirrel-cage rotors

Squirrel-cage rotors comprises of rotor bars to form a cylindrical cage. Terminal windings are short circuited by using short-circuit-rings. The total number of phases $m_2 = N_2$. It is designed in such a way that rotor windings does not have any access while operating, which results in a missing opportunity to directly influence the operational behaviour as shown in figure 2.5 (a).

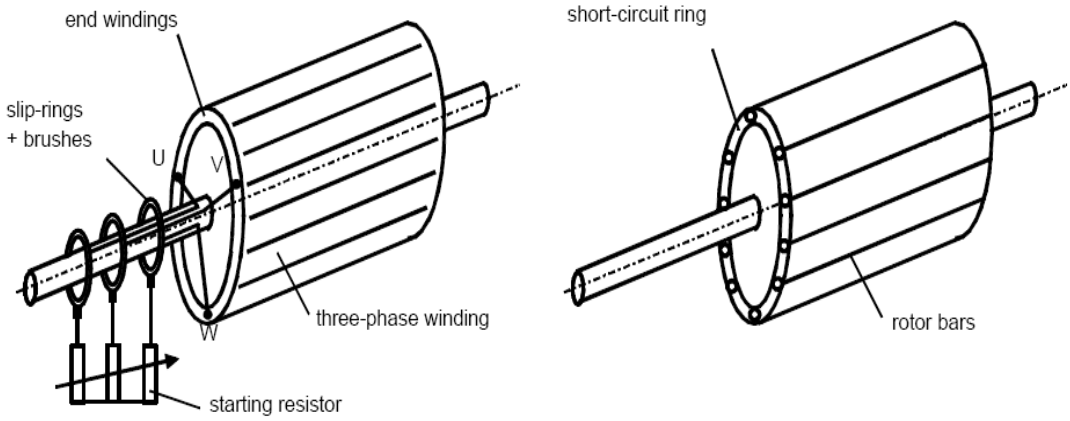

Figure 2.5 (a) Induction machine, rotor type overview (Henneberger, 2002)

Stator slots of a three phase symmetric winding are placed such that they are connected in star or delta-connection. Similarly rotor slots also contain the same connection which is short circuited. The windings of the machines is designed with number of pole pairs greater than one (p>1) distributed on more than one slot q>1.

The best example is 6 stator slots per pole pair (Henneberger, 2002).When the IM is bypassed by three-phase networks of frequency f_1, this produces balance currents to create the rotating field when the motor starts rotating with synchronous speed n_1. This field induces a current of frequency f_2 inside the conductors of the rotor windings. When the induction machine are supplied by three-phase networks of frequency f_1, produces balanced currents. To generate a rotating field inside the air gap between stator and rotor revolving with synchronous rotational speed of n_1.

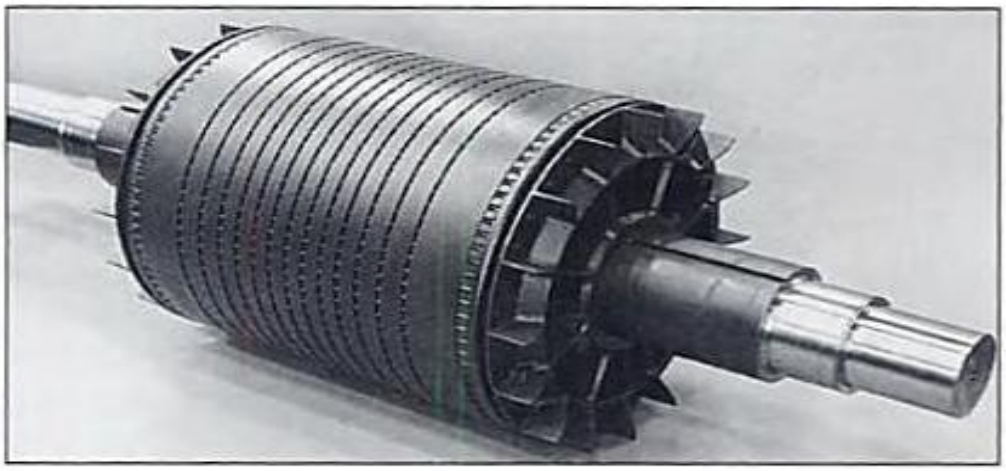

Fig 2.5 (b) Sketch of cage rotors (Stephen, 2005)

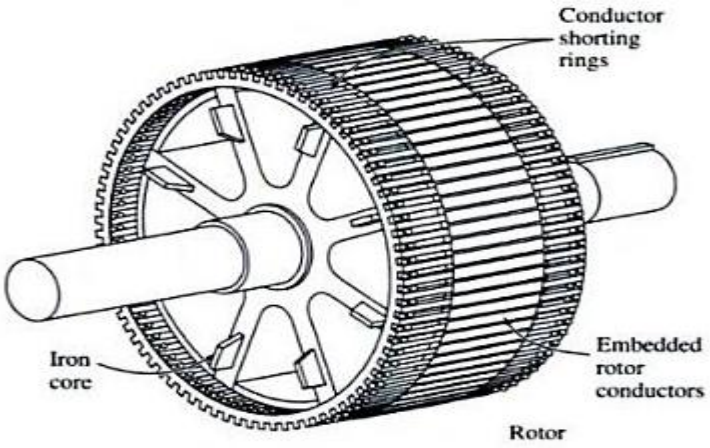

Figure 2.5 (c) A Typical cage Rotor (Courtesy of General Electric company) (Stephen, 2005)

Later these field induces currents of frequency f_2 inside the rotor conductors and also creates another field which is revolving with different speed n_2 relatively towards the rotor speed n and relatively towards the stator field with $n_1=n+n_2$, Due to *Lenz's Law* **(**is defined as an induced current is always in such a direction as to oppose the

motion or change causing it), rotor currents counteract their origin, which is based on relative motion between rotor and stator. Thus rotor currents and stator field revolves with synchronous speed which ultimately generates torque in the direction of the stator field and try to match speed with stator field.

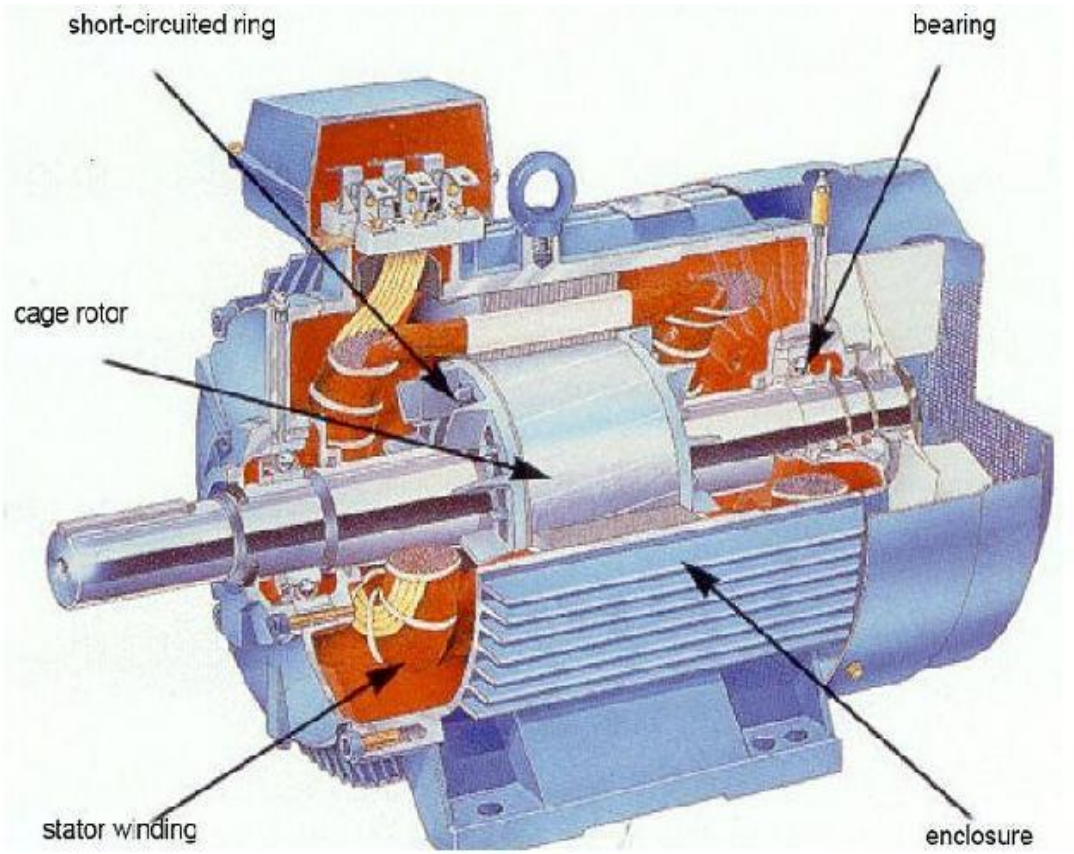

Figure 2.6 Induction machine, general design (Henneberger, 2002)

If the relative motion between stator and rotor field is not up to the mark induction effect may disappear in that case rotor will not reach stator field. At that point rotor show slips against the stator field which is termed as asynchronous. Torque is directly proportional to slip (Henneberger, 2002). The general design of an IM is shown in figure 2.6

Synchronous speed $n_1=f_1/p$

Rotor speed n

Slip $s= n_1-n/n_1=f_2/f_1$

2.4 Different types of Induction Machine (IM)

The similarity of synchronous machine and induction machine is both have same physical stator with different rotor winding respectively Stephen (2005). As we discussed above that there are two different types of IM rotors which is inscribed in the stator as shown in figure 2.7.and different pars of rotor is shown in the figure 2.8

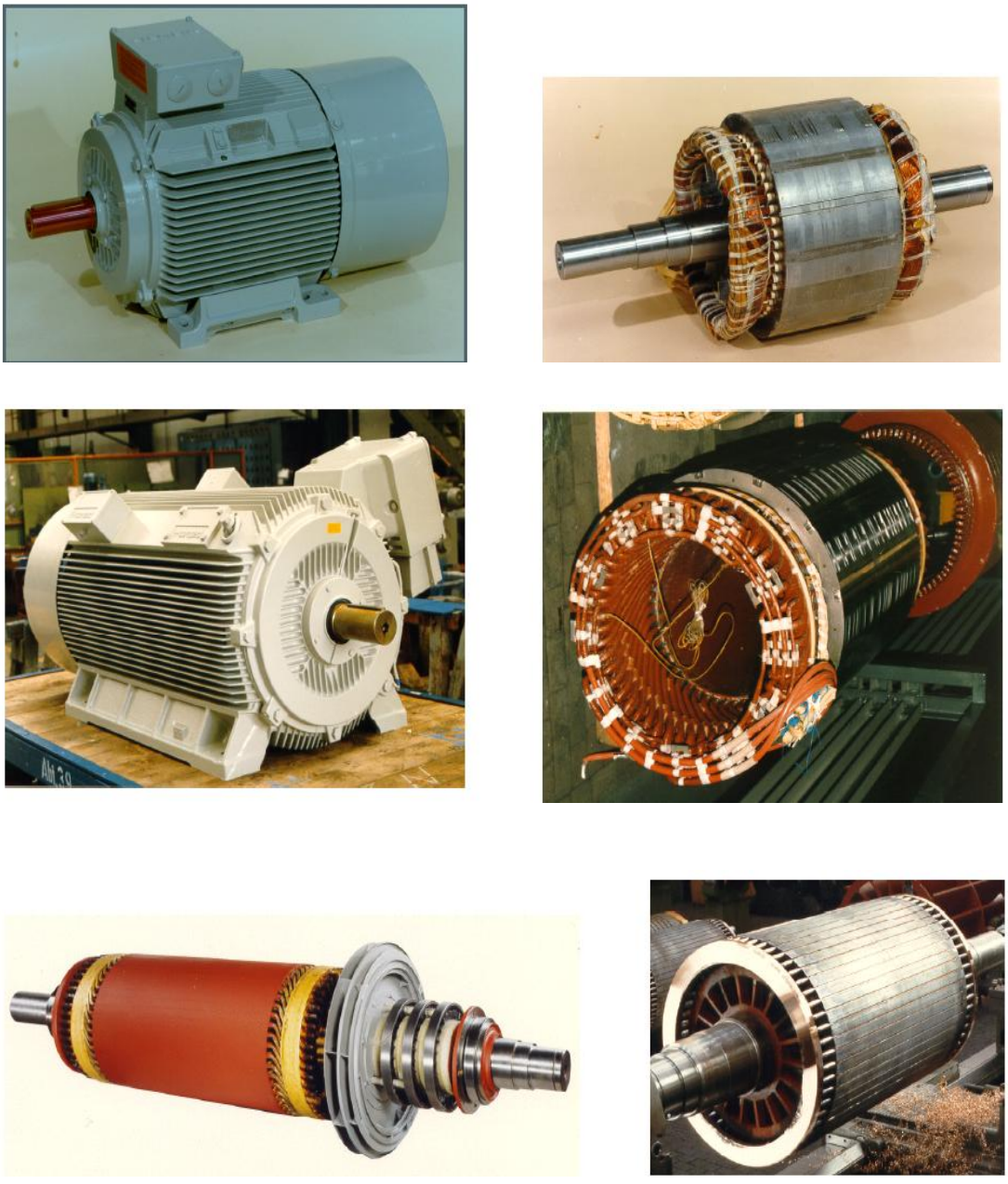

Fig. 2.7 high-voltage induction motor, power: 300 kW (Siemens) - case with shaft (upper left), stator (upper right), slip-ring rotor (lower left), squirrel-cage rotor (lower right (Henneberger, 2002)

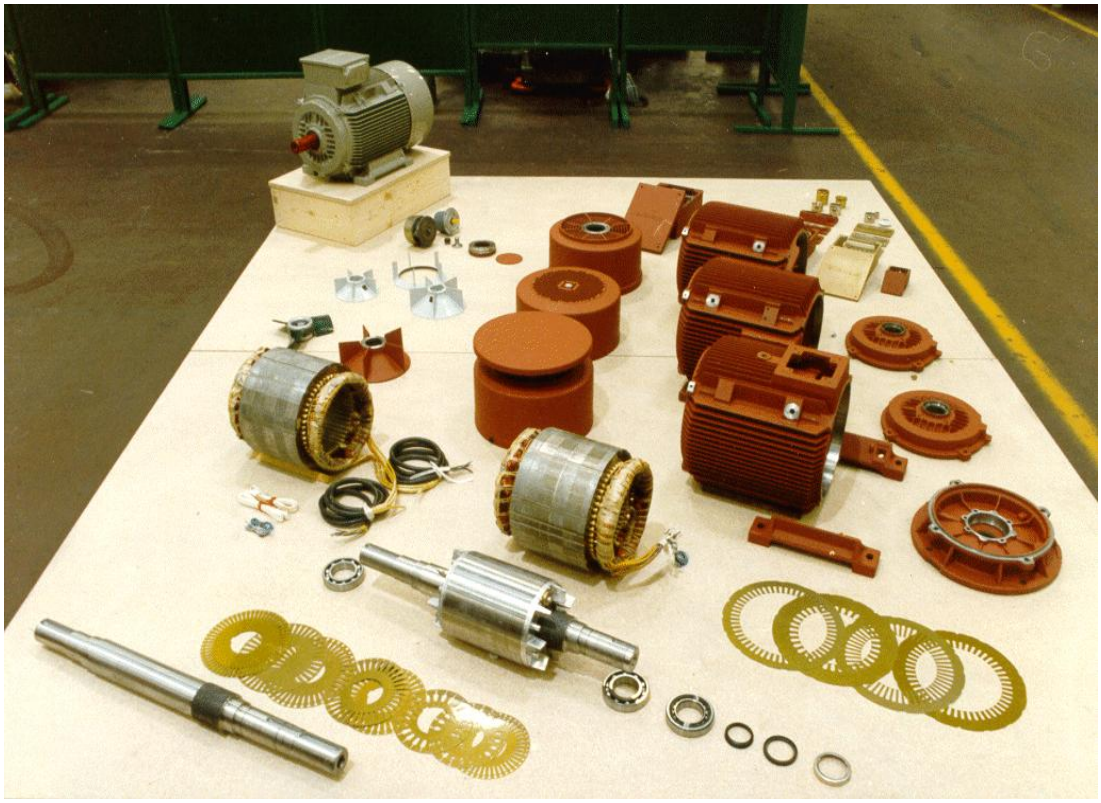

Figure 2.8 Induction machine unassembled parts (Henneberger, 2002)

2.4 (a) Wound rotor Induction Machine (IM)

The second type is wound rotor IM. The windings of the stator and rotor is similar to each other.In general, the 3-phases windings of the rotor are star connected and at the ends of the three rotor wires are tied to slip rings on the rotor's shaft. The windings of the rotor are shorted through riding on the slip rings.(Humphries, 1988) The wound-rotor induction motorhas a stator essentially the as a squirrel cage inductionmotor as shown in figure 2.9. The difference is in the rotor, the Torque-speed charactecristics of the motor can be improved by adding extra resistance which is inserted into the rotor circuit.

Wound Rotor induction motor is rarely used because it's more expensive compare to cage rotor and requires lot of maintaines.

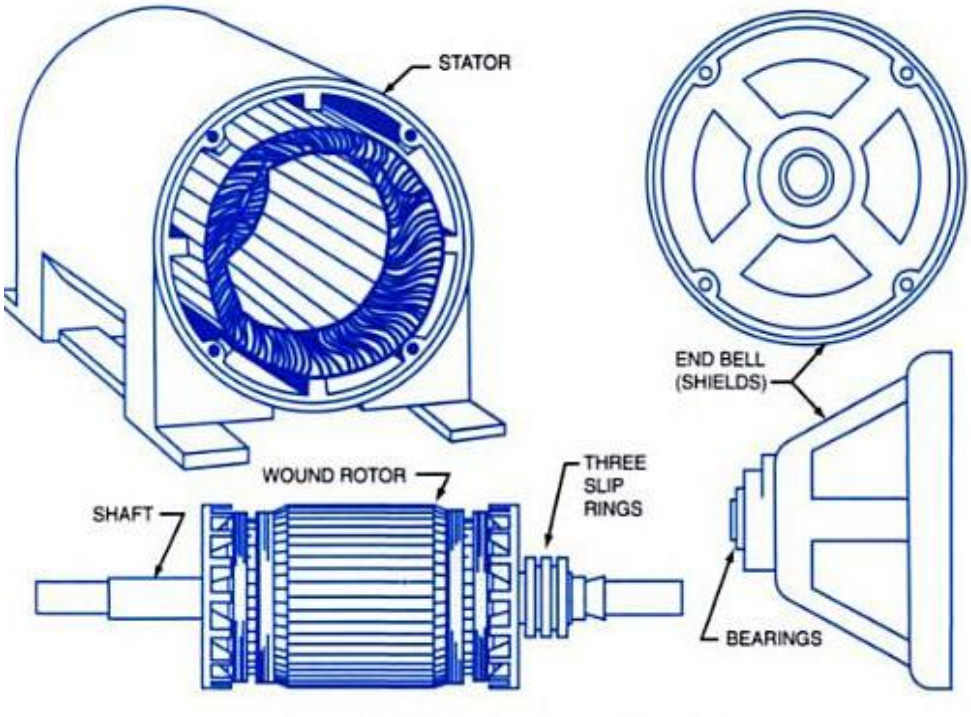

Fig 2.9 Parts of Wound-Rotor motor (Walter, 2001)

2.5 Literature Review

(Bose, 1998) From the past two decades many researchers published papers to explain various method of estimation of rotor flux, speed, and torque so on. In general, estimation can be done by implementing Fuzzy logic or by Luenberger observer, the model reference adaptive scheme, and the extended kalman filter (EKF). Fuzzy logic is a part of our project, which helps us to a wide extent to achieve our simulation. According to Bose describes a *quasi-fuzzy* method estimation stator-resistance of an induction motor, stator-resistance value can be derived from winding temperature estimation as a function of frequency and stator current by designing a mathematical model of the machine. Sensor less vector control of induction motor plays an important role in our project, the estimation of flux vector, speed and frequency for both stator and rotor oriented vector control methods, which are based on voltage model because of variation in stator resistance the computation of voltage control method is not accurate. At zero frequency (i.e., speed) the error is incompatible to solve Bose (1998). This inaccurate flux vector

gives error in both magnitude and phase of flux of an induction motor drive. The impact of the error crosses the limit by affecting the direct torque control (DTC). The stator-flux-oriented direct vector control can be solved because it is directly proportional to stator resistance variation.

(Busawan et al., 2001) summarises that a nonlinear observers for the estimation of the rotor flux and the load torque in an induction motor. The observers are designed on the basis of the standard α - β Park's model (Busawan et al., 2001). Where as (Holtz, 2003) explains about the performance of sensor less controlled induction motor is poor at very low speed. To overcome this drawback, a pure integrator is employed for stator flux estimation. The time-variable dc offset voltage is estimated from the flux drift in a parallel stator model. Vector controlled induction motor without speed has taken an advantage. The absence of the mechanical speed reduces cost and volume of the drive motor. This can be achieved using only sensor cable which increases the reliability of the overall system. Even though there is a problem to achieve robust sensor less control at very low speed at zero stator frequency. In general, all the estimation methods are one ways are the other related rotor induced voltage which makes a stator frequency reduces to zero. This problem can be eliminated by subjecting continuous high-frequency signal into the stator winding or else by exploiting the transient excitation caused by the switching of the PWM inverter. Many researches have been done to improve the fundamental model for flux estimation. The phase angle vector is also termed as *field angle* δ. The field angle enables the transformation of the stator current vector into field coordinates, thus making the electromagnetic torque and the flux of the machine independently controllable (Holtz, 2003).

(Robyns et, al., 1998) illustrates the indirect field control to reduce its sensitivity to parameter uncertainties can be done by applying a simple fuzzy logic block to ensure the field orientation. Generally for the high performance motion control induction actuators requires control the flux and current producing the torque. While measuring the flux in an induction actuator has following drawbacks i.e. flux is often indirectly controlled by controlling and intermediate variable, which is along d-axis of the stator current and the rotor flux along the q-axis which is equals to zero. Since it’s dependent on the actuator model, the flux control method is sensitive to electrical

parameter uncertainties. Fuzzy logic is used to reduce the sensitivity of the flux orientation to the parameter uncertainties and also for the variation purpose in the indirect field oriented control strategy. Fuzzy logic is used for determining the flux orientation by adding two different methods. The design of the fuzzylogic block emphasizes on a theoretical analysis of the flux control sensitivity to parameter uncertainties (Robyns et, al., 1998).

(Rehman, 2008) explains about direct field-orientation motor drive system by considering two aspects i.e. SMVMFO (Sliding mode voltage mode flux observer) and FMRLV (Fuzzy model Reference learning controller). The speed of the induction motor is regulated using an FMRLV and the rotor flux estimation for the direct field orientation (DFO) is analyses by SMVMFO. The field-oriented control of AC machines provides a high performance torque control. Field-oriented control can be explained by two ways i.e. direct field orientation (DFO) and indirect field orientation (IFO). DFO is a closed-loop feedback system based on the rotor flux estimation where as IFO is an open-loop feedback system based on the rotor slip calculation. In some special cases DFO is preferred over IFO because it is less sensitive to rotor time constant. Terminal quantities-based flux observers designed in the past is sensitivity to electrical parameter uncertainties. Rehman (2008) various techniques have been launched to improve the rotor flux estimation such as luenberger observer, Model reference scheme and EKF. Model reference adaptive schemes are proposed in where one of the flux estimators acts as a reference model, and the other acts as the adaptive estimator.

Furthermore, (Wang et al., 2008) highlights that Speed sensor less field-oriented vector control of induction motor depends on effective estimation of rotor flux. In the voltage model based flux estimation, a low pass filter (LPF) is normally used to replace the pure integrator to avoid integration drift and saturation problems. However, the LPF estimator may introduce magnitude and phase errors, and results in degraded estimation performance at low operating frequency. The flux estimation error is compensated according to feedback signal of the estimated flux. To achieve the compromise, an improved programmable LPF rotor flux estimator with a compensator for dc drift restraint is introduced. (Bartolo et al., 2008) explains general principles of saliency tracking in AC machines. Special attention is given to

pulse type injection for the extraction of a rotor or flux position signal. The saliency is tracked by measuring the current derivative resulting from voltage 'test' vector application. (Hakiki et al., 2007) A nonlinear sliding flux was proposed for an induction motor. Its dynamic observation errors converge asymptotically to zero, independently from the inputs. The dynamic performance of this sliding observer was compared to that of Verghese observer via a simulation of an IM driven by U/F control in open loop. Lian (2006) describes the fuzzy observer of the induction motor is simply constructed to estimate the immeasurable states of rotor speed and rotor flux, where the estimation gains are obtained by solving a set of linear matrix inequalities.

Hilairet et al., (2009) illustrates that the methods can be placed into two different classes. The first method consists of estimating the stator harmonic frequencies produced by the rotor saliency when the rotor turns digital signal processing (DSP) estimators retrieve the current which contain the encoded speed. This approach has been used frequently because of high accuracy estimation in the steady state. But this method suffers from speed tracking error during transient state and results are poor. Hilairet et al., (2009) describes the second method is based on the rotor back electromotive force (EMF) which contains the velocity information. Non-linear state observers such as extended Luenberger observers can be used to estimate this back EMF from the stator currents and voltages Hilairet et al., (2009). These observers depend on parameter variations. The second method gives accurate speed estimation during both transient and steady states. Computational cost is generally considered as a major shortcoming of the Kalman filters used for flux and velocity estimation of AC motors (Hilairet, *et al.*, 2009). Hilairet *et al.*, (2009) presented an effective implementation of an extended Kalman filter used for the estimation of both rotor flux and rotor velocity of an induction motor, the problem of estimating the state, parameters and unknown inputs generally leads to an augmented state system that is commonly treated with an augmented state Kalman filter, whose implementation is in practice computationally intensive. To reduce the computational cost, Friedland (1969) introduced, for the first time a two-stage Kalman estimator. The main idea is to decouple the Kalman filter into two parallel filters: a full-order filter and another one for the augmented state. Friedland's filter is devoted to estimating the state of a linear process in the presence of a constant but unknown bias vector. Related works

are Hsieh and Chen (1999), Ignagnim (2000), Keller (1997), Keller and Darouach (1999), Kim, Jee, and Song (2008) and Tanaka (1975).

To implement the control law for induction motors based on rotor flux control requires estimation of modulus and phase of the rotor flux vector in the stationary mode. The rotor flux components can be estimated either by the desired frame Alonge (2007)

1) Open loop observers, such as current and voltage models.
2) Closed loop observers, such as full and reduced order (Alonge, 2007).

Guergazi et al., (2007) asserts that in relation to rotor speed**,** flux and resistance of estimation in an induction motors, EKF are widely used rather than linear one. Because it is a well-known fact that rotational speed and rotor resistance cannot be estimated simultaneously if the machine is fed through a three-phase sinusoidal voltage source at the fundamental frequency. (Zhang, 2008) presents a new rotor flux estimation algorithm using neural network for induction motor, based on the left-inversion method. Using the standard fifth-order model of the three-phase induction motor in a stationary two axes reference frame, the flux *assumed inherent sensor* is constructed and its left-invertible is validated. The Artificial Neural Network (ANN) left-inversion flux estimator is composed of two relatively independent parts - a static ANN used to approximate the complex nonlinear function and several differentiators used to represent its dynamic behaviours, so that the ANN left-inversion is a special kind of dynamic ANN in essence.

Jin et al., (2006) explains that an adaptive rotor flux estimator based on model reference adaptive approach was proposed to accurately estimate the flux of induction motors in modern high-performance drivers. Using an induction motor as the reference model and a group of observed data equations as adjustable system, a model reference adaptive system (MRAS) was established to estimate the rotor flux of the induction motor and identify the motor parameters online during operation. The adaptive laws of parameters were designed and the flux estimator was proved convergent. Blaabjerg et al (2005) outlines alternative methods of estimation. There are two flux and three rotor speed estimators, which were chosen from the most promising methods presented in literature. Hemsas et al., (2005) describes the use of

Artificial Neural Networks and Neuro-Fuzzy Networks for the simultaneous estimation of the speed, rotor flux and rotor resistance of an induction motor.

Caruana et al., (2003) describes a new approach to the tracking of the flux position saliency of an induction machine by means of high-frequency (HF) signal injection in the synchronous rotating frame. A modified scheme is proposed in which a rotating HF field is established in the d-q rotating reference frame. The scheme enhances the performance of harmonic elimination methods to reduce the effects of secondary saliencies. A new harmonic elimination method is introduced based on the Kalman filter. Medvedev (1994) Design aspects of a flux observer for induction machines are discussed. By making use of a second-order, complex-valued, state-space model of the induction machine dynamics, a stability criterion and observer estimation error bounds are obtained. Macek-Kaminska (1996) states that the problems connected with the mathematical modeling of the squirrel-cage induction motors are either high or low power. The most suitable mathematical model for the simulation of dynamics and statics of that type of machines and the method of the estimation of the parameters of that model are presented. The elaborated method is versatile. It enables the calculation of the parameters on the basis of the measured static characteristics or dynamic runs.

(Zheng, 1999) explains that an adaptive estimator for rotor resistance to simultaneously estimate fluxes and rotor speed for an induction motor is designed with the assumption that only stator currents are measurable. The basic idea is to build up a stable adaptive observer and treat rotor speed and rotor resistance as slowly varying unknown parameters in the framework of MRAS. Sun et al., (1999) In order to estimate the rotor flux of an induction motor accurately and to achieve a high vector control performance, two estimation models based on artificial neural networks are presented. Two networks are employed in series in one model, and coupled in the other. Alonge (2007) clarifies simple and effective design criteria of rotor flux reduced-order observers for motion control systems with induction motors. While the observer is optimized for rotor and stator resistance variations, a sensitivity analysis is carried out in the presence of variations of all the motor parameters by means of either transfer function from true to observed rotor flux or simulation in a Matlab-simulink environment, assuming the voltages supplying the

motor to be different from those supplying the observer. The sensitivity analysis makes it possible to establish design criteria for the observer in question. The behavior of the proposed reduced order observer is compared with current model and voltage model observers (Alonge, 2007).

(Kouz et al., 2009) describes the analysis and design of fuzzy SMSO (sliding-mode speed observer) applied to vector control of an induction motor. By introducing the FSMO (fuzzy sliding-mode speed observer) gain of the SMO and chattering phenomenon due to switching surface. The FSMO estimates rotor speed and flux and retains the membership sets of symmetrical triangular shape. By introducing dynamic model the main features of the proposed observer are investigated and compared with SMO.

(Ta-cao, 1996) describes by implementing the fuzzy logic rotor resistance and speed can be determined in indirect vector-controlled induction motor drive. A model-reference adaptive scheme is then proposed in which the adaptation mechanism is executed using fuzzy logic. To achieve decoupling control of torque and flux, estimator of fuzzy logic rotor resistance is designed.

(Orlowska-Kowalska, 2007) expresses a model reference adaptive control speed control (MRAC) using on-line trained fuzzy neutral network (FNN) was applied to the sensor less induction motor drive system. PI-type fuzzy logic controller is used as the speed controller. The rotor flux and speed of vector controlled induction motor was estimated using the full-order state observer and speed estimator.

2.6 Fuzzy Logic

In the present era where number of papers published daily about different topics such as design and simulation fuzzy was one of them however some of the earlier controversies regarding the applicability of fuzzy logic have solved, there are still influential voices which are critical and/or sceptical. Some people trying to prove that fuzzy logic is wrong (Bose, 2002).The term “fuzzy logic” can be explained in two ways i.e. *wide and narrow.* In a narrow sense, fuzzy logic is a logical system,

which is an extension of multivalued logic. But in a wider sense, which is in predominant use today, fuzzy logic (FL) is almost synonymous with the theory of fuzzy sets, a theory which relates to classes of objects with unsharp boundaries in which membership is a matter of degree which was discussed in chapter 4. What is important to recognize is that, even in its narrow sense, the agenda of fuzzy logic is very different both in spirit and substance from the agendas of traditional multivalued logical systems.(1) fuzzy logic is a broad theory including fuzzy set theory, fuzzy logic, fuzzy measure so on. Fuzzy set theory is an extension of conventional set theory. Fuzzy logic is an extention of conventional (binary) logic (Bose, 2002).

2.7 Fuzzy sets

(Bose, 2002) Fuzzy logic mainly deals with complex issues which are incorporated with fuzziness or vagueness. Fuzzy logic uses Boolean logic set theory. Fuzzy set theory based on fuzzy logic, a Particular object has a degree of membership in a given set that may be anywhere in the range of 0 to 1 because of this reason called as Multi-valued logic (0 to 1). Form the figure 2.10, describes as fuzzy logic problem consists of input/output, static, nonlinear mapping problem through a “Black Box” input space is used to process the input information and send through the output via black box.

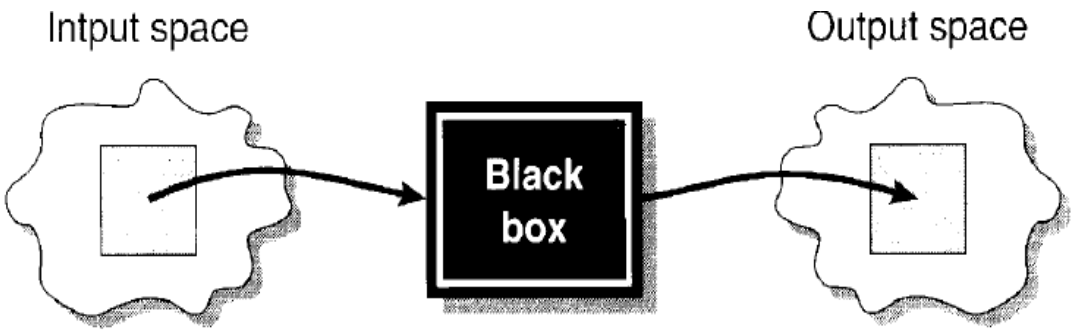

Figure 2.10 Input/output mapping problem (Bose, 2002)

Generally, mapping can be in dual form i.e. static and dynamic and its characteristic is similar to black box's characteristics. The black box plays a vital role in sending the solution to the output.

2.8 Membership Functions

A membership function (MF) is a curve that defines how each point in the input space is mapped to a membership value (or degree of membership) between 0 and 1. The input space is sometimes referred to as the universe of discourse, a fancy name for a simple concept. A MF can have different shapes, as shown in Fig. 2.11. The simplest and more commonly used MF is the triangular-type, which can be symmetrical or asymmetrical in shape. A trapezoidal MF has the shape of a truncated triangle. Two MFs are built on the Gaussian distribution curve: a simple Gaussian curve and a two-sided composite of two different Gaussian curves. The bell MF with a flat top is somewhat different from a Gaussian function. Both the Gaussian and bell functions are smooth and non-zero at all points. A sigmoidal-type MF can be open to the right or left. Asymmetrical and closed MFs can be synthesized using two sigmoidal functions, such as difference sigmoidal and product sigmoidal.

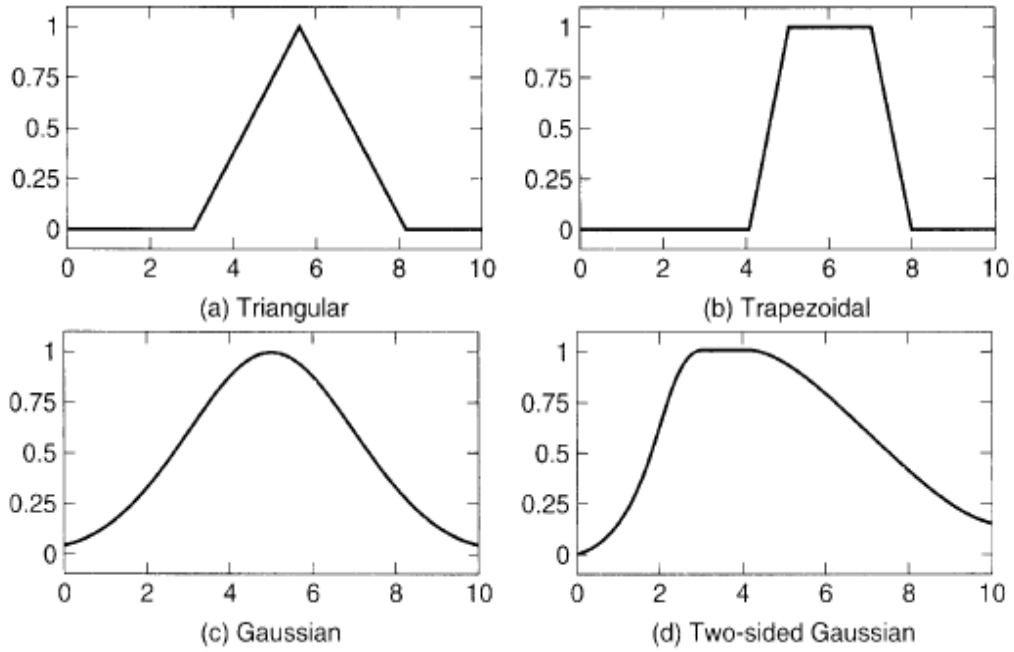

Figure 2.11 Different types of Membership functions (Bose, 2002)

Chapter 3 Dynamic model of the induction machine

In the Previous chapter, we have discussed the basic principals of rotating field of the IM, different types of IM and design, working. It is crucial to start with good and appropriate reviews which were verified by numerous journals. However, (Busawan et al., 2001) summarises that a nonlinear observers for the estimation of the rotor flux and the load torque in an induction motor. The observers are designed on the basis of the standard α - β *Park's model.*

3.1 Introduction

To understand the design of vector control drives of an induction machine, dynamic/mathematical model plays an important role. By considering various assumptions IM can be controlled in a precise/accurate way and dynamic model is the best example for assumption. Nevertheless, the model should incorporate all the important dynamic effects occurring during both steady state and transient operations. In addition to that, the assumptions should make some sense for any changes in the inverter's supply for currents and voltages (Bose, 2002).

This kind of dynamic model can be obtained by two ways

(a) Two-axes theory and

(b) Space vector phasor theory.

Despite the compactness and the simplicity of the space phasor theory, both methods are actually close to each other (Bose, 2002). The following assumptions were made when the motor is subjected to dynamic model.

(a) Symmetrical two-pole, three phase windings.

(b) The slotting effects are neglected.

(c) The permeability of the iron parts is infinite.

(d) The flux density is radial in the air gap.

(e) Iron losses are neglected.

(f) The stator and the rotor windings are simplified as a single, multi-turn full pitch coil situated on the two sides of the air gap (Bose, 2002).

The following points should be kept in mind before constructing dynamic model of an induction motor.

(a) To control the dynamics of the drive system, dynamic behaviour of the IM is primary.

(b) Dynamic behavior of IM can be described by using dynamic model of IM.

(c) Dynamic model increases complexity because of magnetic coupling between stator and rotor phases.

(d) Coupling coefficient is directly proportional to rotor position which in turn directly related to time.

(e) Dynamic behaviour of IM can be described by differential equations with time varying coefficients (Bose, 2002).

3.2 Need for Dynamical modelling of Induction Motor

The per-phase equivalent circuit of the machine is only valid in steady-state condition. Unlike in transient state, electrical transients are neglected during load changes and variation in stator frequency when subjected to steady state condition. For adjusting the speed drive system, the machine is connected with feedback loop, therefore transient state comes into picture. Besides, high-performance drive control, such as vector or field-oriented control is based on the dynamic d-q model of the machine. Therefore, to understand basic principles of vector control, a good understanding of the d-q model is necessary (Bose, 2002).

3.3 Dynamic d-q Model

(Bose, 2002) The dynamic performance of an induction and synchronous machine is difficult to judge because the three-phase rotor windings move with respect to the stator windings as shown in figure 3.1(a).

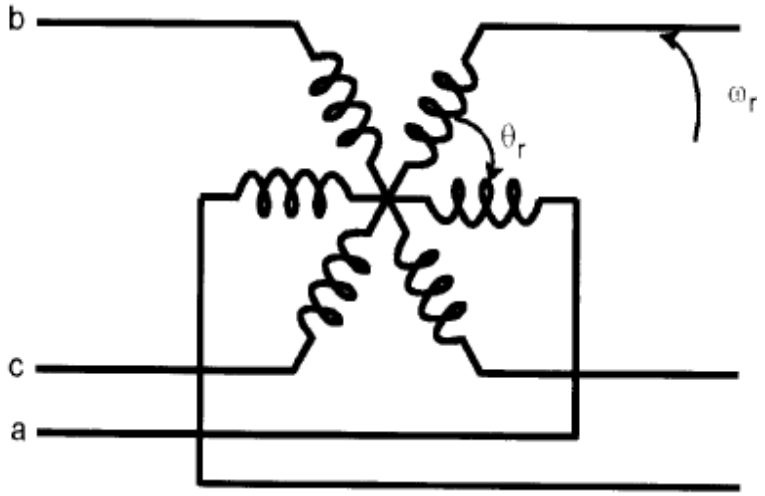

Figure 3.1 (a) Coupling effect in three-phase (Bose, 2002)

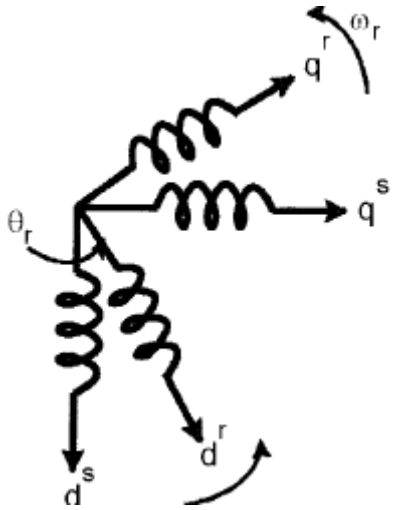

Figure 3.1 (b) Equivalent two-phase machine (Bose, 2002)

The three-phase windings of the transformer and induction motor is similar to each other in which coupling coefficients between the stator and rotor phases change continuously with the change of rotor position θ_r.

In general, there are number of methods in which induction machines are presented the one is through differential equations with time-varying mutual inductances, but with this method complexity increases. The three-phase machines can be represented by a two phase machine as shown in figure 3.1(b), where d_s-q_s correspond to stator direct and quadrature axes, and d_r-q_r correspond to rotor direct and quadrature axes respectively (Bose, 2002).

In 1920, R.H. Park introduced a new theory to overcome this problem by formulating a change of variables i.e. current, voltage and flux linkages associated with the stator windings of the synchronous machine with variables associated with fictitious windings rotating with rotor at synchronous speed. He shifts the stator variables to a synchronously rotating reference frame fixed in the rotor. This kind of transformation is named as *park's transformation*; he then showed that all the time-varying inductances that occur due to an electric circuit in relative motion and electric circuits with varying magnetic reluctances can be eliminated. Bose, (2002) later on, in 1930 Stanley showed that time-varying inductances in the voltage equations of the induction machine due to electric circuits in relative motion can be eliminated by transforming the rotor variables to variables associated with fictitious stationary windings. In this case, the rotor variables are transformed to a stationary reference frame fixed on the stator.

G.Kron proposed a transformation of both rotor and stator variables to a synchronously rotating reference frame that moves with the rotating magnetic field. D.S.Brereton proposed a transformation of stator to a rotating reference frame that is fixed on the rotor. In fact, it was shown later by Krause and Thomas that time-varying inductances can be eliminated by referring the stator and rotor variables to a common reference frame which may rotate at any speed (arbitrary reference frame) (Bose, 2002).

3.3 (a) Axes transformation

(Bose, 2002) Consider a symmetrical three-phase IM with stationary as-bs-cs axes at $2\pi/3$ angle apart, as shown in figure 3.2. Our aim is to transform the three-phase stationary reference frame (as-bs-cs) variables into two–phase stationary reference frame (d^s-q^s) variables and then these to synchronously rotating reference frame (d^e-q^e) and similarly two-phase stationary reference frame can be transform into three-phase stationary reference frame.

Let us assume that the d^s-q^s axes are oriented at θ angle, as shown in figure 3.2. The voltages $v_{ds}^{\ s}$ and $v_{qs}^{\ s}$ can be resolved into as-bs-cs components and can be represented in matrix form as

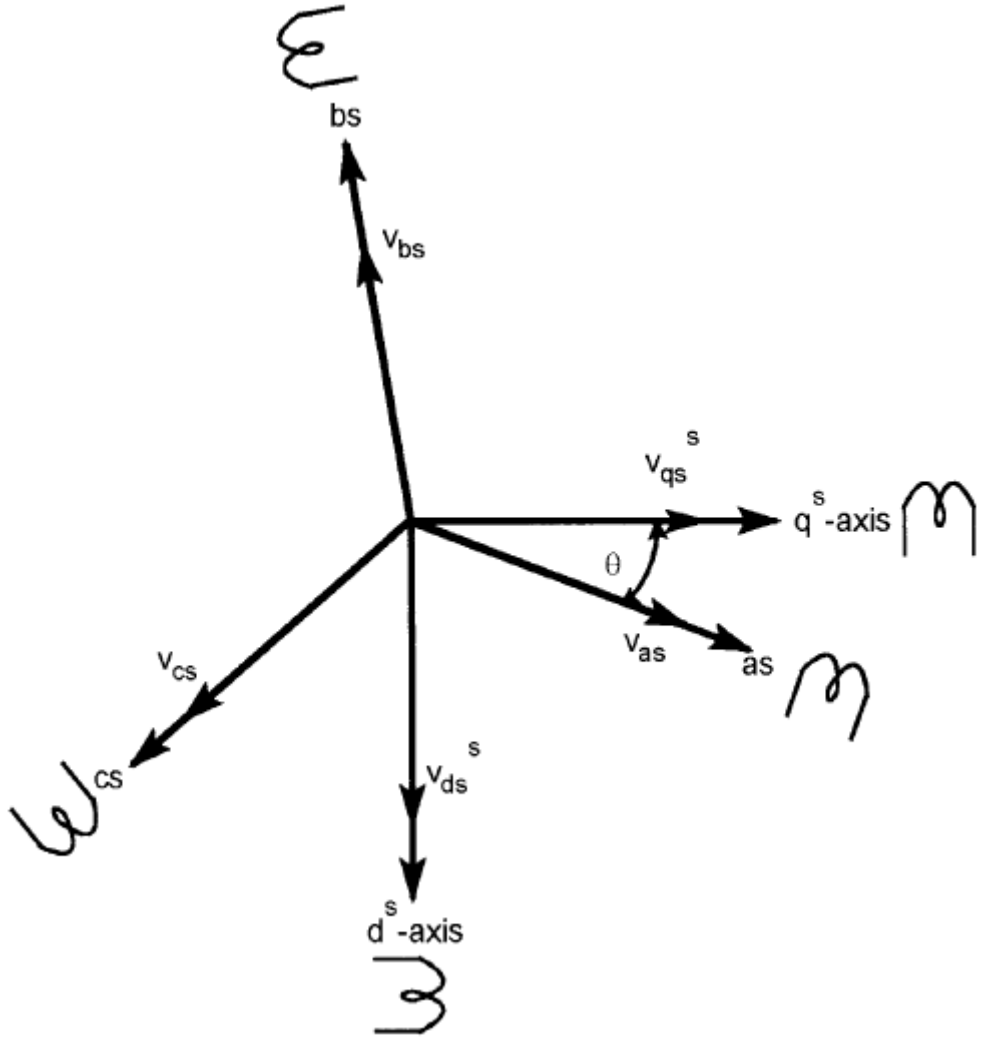

Fig. 3.2 Stationary frame a-b-c to d^s-q^s axes transformation (Bose, 2002).

$$\begin{bmatrix} v_{as} \\ v_{bs} \\ v_{cs} \end{bmatrix} = \begin{bmatrix} \cos\theta & \sin\theta & 1 \\ \cos(\theta-120^o) & \sin(\theta-120^o) & 1 \\ \cos(\theta+120^o) & \sin(\theta+120^o) & 1 \end{bmatrix} \begin{bmatrix} v_{qs}^{s} \\ v_{ds}^{s} \\ v_{os}^{s} \end{bmatrix} \quad (3.1)$$

The corresponding inverse relation is

$$\begin{bmatrix} v_{qs}^{s} \\ v_{ds}^{s} \\ v_{os}^{s} \end{bmatrix} = \frac{2}{3} \begin{bmatrix} \cos\theta & \cos(\theta-120^o) & \cos(\theta+120^o) \\ \sin\theta & \sin(\theta-120^o) & \sin(\theta+120^o) \\ 0.5 & 0.5 & 0.5 \end{bmatrix} \begin{bmatrix} v_{as} \\ v_{bs} \\ v_{cs} \end{bmatrix} \quad (3.2)$$

Where V_{os}^{s} is added as the zero sequence components. By considering voltage as variable. Current and flux linkages can be transformed by similar equations. It is convenient to set θ = 0, so that the q^s-axis is aligned with the

as-axis. Ignoring the zero sequence components, the transformation relations can be simplified as (Bose, 2002).

$$Vas=Vqss \quad (3.3)$$

$$Vbs = -(1/2)Vqss - (\sqrt{3}/2)\,Vdss \quad (3.4)$$

$$Vcs = -(1/2)\,Vqss + (\sqrt{3}/2)\,Vdss \quad (3.5)$$

$$Vqss=(2/3)\,Vas -(1/3)\,Vbs - (1/3)\,Vcs = Vas \quad (3.6)$$

$$\text{And inversely} \quad Vqss=(2/3)\,Vas -(1/3)\,Vbs - (1/3)\,Vcs = Vas \quad (3.7)$$

$$Vdss = -(1/\sqrt{3})\,Vbs + (1/\sqrt{3})\,Vcs \quad (3.8)$$

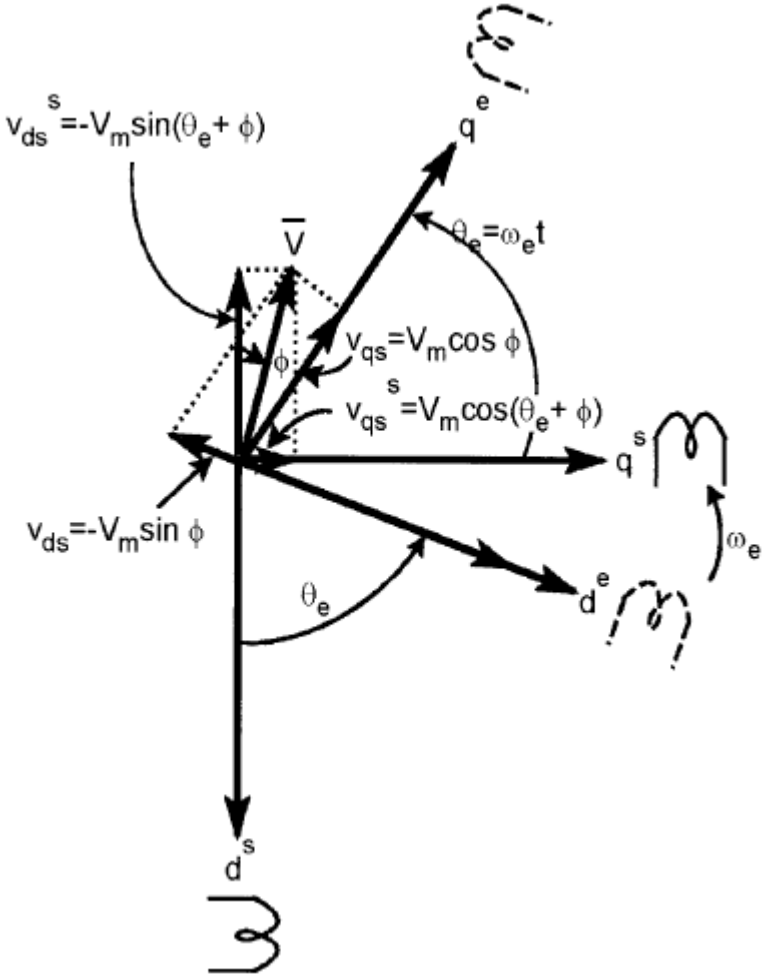

Figure 3.3 Stationary frame d^s-q^s to synchronously rotating frame de-qe transformation (Bose, 2002)

Figure 3.3 Shows the synchronously rotating d^e-q^e axes, which rotates at synchronous speed ω_e with respect to the d^s-q^s axes and the angle $\theta e = \omega_e t$. Two-phase d^s-q^s

windings are transformed into the hypothetical windings mounted on the d^e-q^e axes. The voltages on the d^s-q^s axes can be converted into the d^e-q^e frame.

$$V_{qs} = V_{qs}^{s} \cos\theta e - V_{ds}^{s} \sin\theta e \quad (3.9)$$

$$V_{ds} = V_{qs}^{s} \sin\theta e + V_{ds}^{s} \cos\theta e \quad (3.10)$$

Again, resolving the rotating frame parameters into a stationary frame, the relations are

$$V_{qs}^{s} = V_{qs} \cos\theta e + V_{ds} \sin\theta e \quad (3.11)$$

$$V_{ds}^{s} = - V_{qs} \sin\theta e + V_{ds} \cos\theta e \quad (3.12)$$

3.3 (b) Synchronously rotating reference frame-Dynamic model

(Bose, 2002) For the two-phase machine shown in figure 3.1 (b), we need to represent both d^s-q^s and d^r-q^r circuits and their variables in a synchronously rotating d^e-q^e frame.

Stator equations can be represented as

$$V_{qs}^{s} = R_s i_{qs}^{s} + d\psi_{qs}^{s}/dt \quad (3.13)$$

$$V_{ds}^{s} = R_s i_{ds}^{s} + d\psi_{ds}^{s}/dt \quad (3.14)$$

Where

ψ_{qs}^{s} and ψ_{ds}^{s} are q-axis and d-axis stator flux linkages.

When these equations are converted to d^e-q^e frame, the following equations can be written

$$V_{qs} = R_s i_{qs} + d\psi_{qs}/dt + \omega_e \psi_{ds} \quad (3.15)$$

$$V_{ds} = R_s i_{qs} + d\psi_{ds}/dt - \omega_e \psi_{qs} \quad (3.16)$$

(Bose, 2002) All the variables are in rotating form. The last term in the equations (3.15) and (3.16) ($\omega e\psi ds$, $\omega e\psi qs$) can be defined as speed EMF due to rotation of the axis, when $\omega_e = 0$, the equations get back to its stationary form. Note that the flux linkage in the d^e and q^e axes induces EMF in the q^e and d^e axes with $\pi/2$ lead angle. If

the rotor is stationary, $\omega_r = 0$, the rotor equations for a doubly fed wound rotor machine will be similar to equations (3.15) - (3.16):

$$V_{qr} = R_r i_{qr} + d\psi_{qr}/dt + \omega_e \psi_{dr} \quad (3.17)$$

$$V_{dr} = R_r i_{dr} + d\psi_{dr}/dt - \omega_e \psi_{qr} \quad (3.18)$$

(Bose, 2002) All the variables and parameters are referred to the stator. Since the rotor actually moves at speed ω_r, the d-q axes fixed on the rotor move at a speed $\omega_e - \omega_r$ relative to the synchronously rotating frame. Therefore, in d^e-q^e frame, the rotor equations should be modified as

$$V_{qr} = R_r i_{qr} + d\psi_{qr}/dt + (\omega_e - \omega_r)\psi_{dr} \quad (3.19)$$

$$V_{dr} = R_r i_{dr} + d\psi_{dr}/dt - (\omega_e - \omega_r)\psi_{qr} \quad (3.20)$$

(Bose, 2002) Figure 3.4 shows the d^e-q^e dynamic model equivalent circuits that satisfy equations (3.15) - (3.16) and (3.19) – (3.20). A plus point of using d^e-q^e dynamic model of the machine is that all the sinusoidal variables in stationary frame appear as dc quantities in synchronous frame. The flux linkage equations in terms of currents can be written from figure 3.4 as follows:

$$\psi qs = Lls\ iqs + Lm(iqs + iqr) \quad (3.21)$$

$$\psi_{qr} = L_{lr}\ q_r + L_m(i_{qs} + i_{qr}) \quad (3.22)$$

$$\psi_{qm} = L_m (i_{qs} + i_{qr}) \quad (3.23)$$

$$\psi_{ds} = L_{ls}\, i_{ds} + L_m (i_{ds} + i_{dr}) \quad (3.24)$$

$$\psi_{dr} = L_{lr}\, i_{dr} + L_m (i_{ds} + i_{dr}) \quad (3.25)$$

$$\psi_{dm} = L_m (i_{ds} + i_{dr}) \quad (3.26)$$

Combining the above expressions with (3.15), (3.16), (3.19) and (3.20), the electrical transient model in terms of voltages and currents can be given in matrix form as

$$\begin{bmatrix} V_{qs} \\ V_{ds} \\ V_{qr} \\ V_{dr} \end{bmatrix} = \begin{bmatrix} R_s + SLs & weLs & SLm & weLm \\ -weLs & Rs + SLs & -weLm & SLm \\ SLm & (we - wr)Lm & Rs + SLr & (we - wr)Lr \\ -(we - wr)Lm & SLm & -(we - wr)Lr & Rr + SLr \end{bmatrix} \begin{bmatrix} i_{qs} \\ i_{ds} \\ i_{qr} \\ i_{dr} \end{bmatrix} \quad (3.27)$$

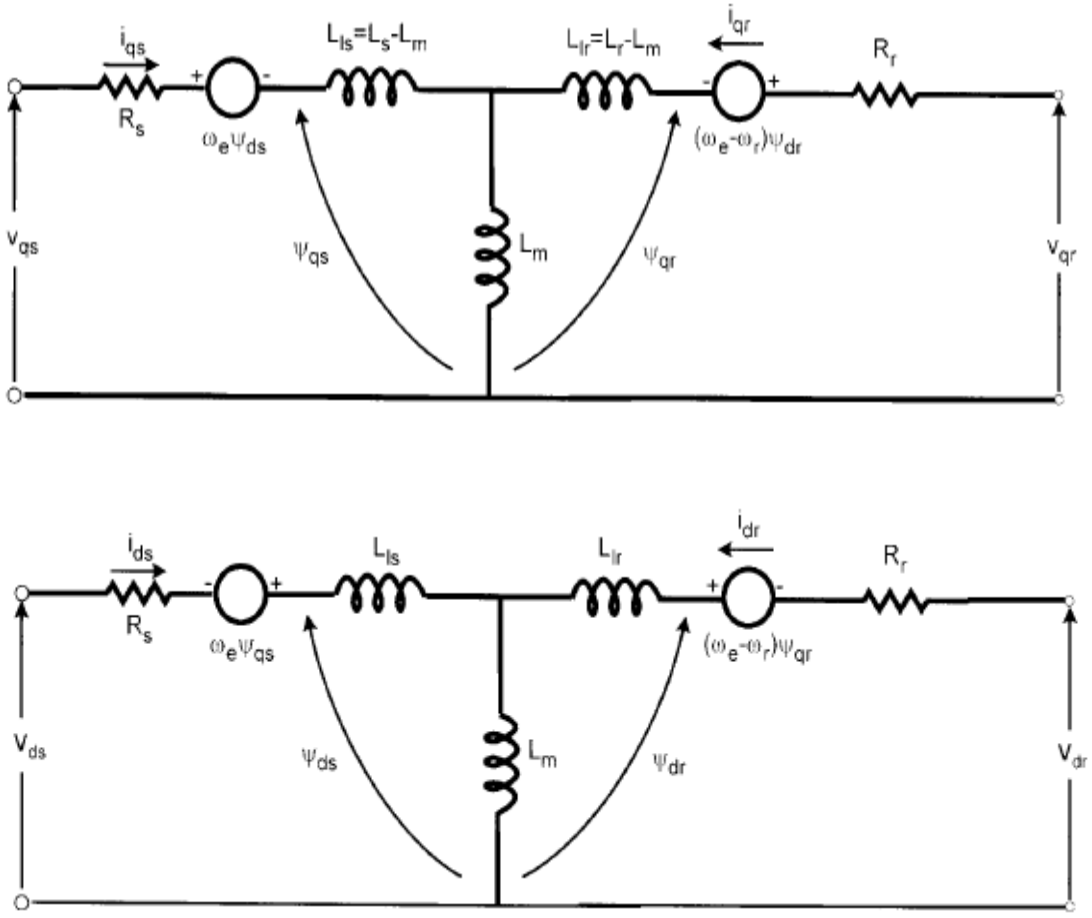

Fig 3.4 dynamic d^e-q^e equivalent circuits of machine (a) q^e-axis circuit, (b) d^e-axis circuit (Bose, 2002)

Where S is the Laplace operator, for a singly-fed machine, such as a cage motor, $v_{qr} = v_{dr} = 0$. If the speed ω_r is considered constant (infinite inertia load), the electrical dynamics of the machine are given by a fourth-order linear system. Then, knowing the inputs V_{qs}, V_{ds} and ω_e, the currents i_{qs}, i_{ds}, i_{dr} and i_{qr} can be solved from equation (3.27). If the machine is fed by current source i_{qs}, i_{ds} and ω_e are independent. Then, the independent variables V_{qs}, $V_{ds,}$ i_{dr} and i_{qr} can be solved from equation (3.27). The speed ω_r in equation (3.27) cannot be normally treated as a constant. It can be related to the torques as (Bose, 2002).

$$Te = T_L + J\, d\omega_m/dt = T_L + (2/P)\, J\, d\omega_r/dt \qquad (3.28)$$

Often, for compact representation, the machine model and equivalent circuits are expressed in complex form. Multiplying Equation (3.16) by –j and adding with equation (3.15) gives

$$V_{qs} - jv_{ds} = Rs(i_{qs} - ji_{ds}) + d(\psi_{qs} - j\psi_{ds})/dt + j\omega_e(\psi_{qs} - j\psi_{ds}) \quad (3.29)$$

Or

$$V_{qds} = R_s i_{qds} + d(\psi_{qds})/dt + j\omega_e \psi_{qds} \quad (3.30)$$

Where V_{qds} and i_{qds} etc. are complex vectors. Similarly, the rotor equations (3.19) – (3.20) can be combined to represent

$$V_{qdr} = R_r i_{qdr} + d\psi_{qdr}/dt + j(\omega_e - \omega_r)\psi_{qdr} \quad (3.31)$$

Figure 3.5 shows the complex equivalent circuit in rotating frame where $v_{qds} = 0$. Note that the steady-state equations can be always be derived by substituting the time derivative components to zero. Therefore from equations (3.30) – (3.31) the steady-state equations can be derived as

$$V_s = R_s I_s + j\omega_e \psi_s \quad (3.32)$$

$$0 = (R_r/S)I_r + \omega_e \psi_r \quad (3.33)$$

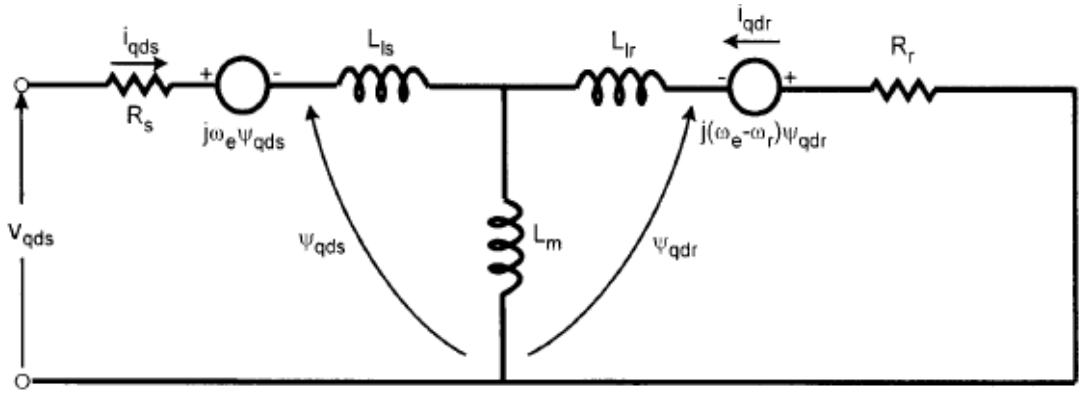

Fig 3.5 Complex synchronous frame dqs equivalent circuit (Bose, 2002)

Where the complex vectors have been substituted by the corresponding rms phasors. These equations satisfy the steady-state equivalent circuit of the induction motor if the parameter R_m is neglected (Bose, 2002).

From equation $T_e = (3/2)(p/2)\hat{\psi}_m I_r \sin\delta$, the torque can be generally expressed in the vector form as(Bose, 2002).

$$T_e = (3/2)(p/2)\psi_m * I_r \quad (3.34)$$

Resolving the variables into d_e-q_e components, as shown in figure 3.6

$$T_e = (3/2)(p/2)\ (\psi_{dm}I_{qr} - \psi_{qm}I_{dr}) \quad (3.35)$$

Several other torque expressions can be derived easily as follows:

$$T_e = (3/2)(p/2)\ (\psi_{dm}I_{qs} - \psi_{qm}I_{ds}) \quad (3.36)$$

$$= (3/2)(p/2)(\psi_{ds}I_{qs} - \psi_{qs}I_{ds}) \quad (3.37)$$

$$= (3/2)(p/2)L_m(i_{dr}i_{qs} - i_{ds}i_{qr} \quad (3.38)$$

$$= (3/2)(p/2)(\psi_{dr}I_{qr} - \psi_{qr}I_{dr}) \quad (3.39)$$

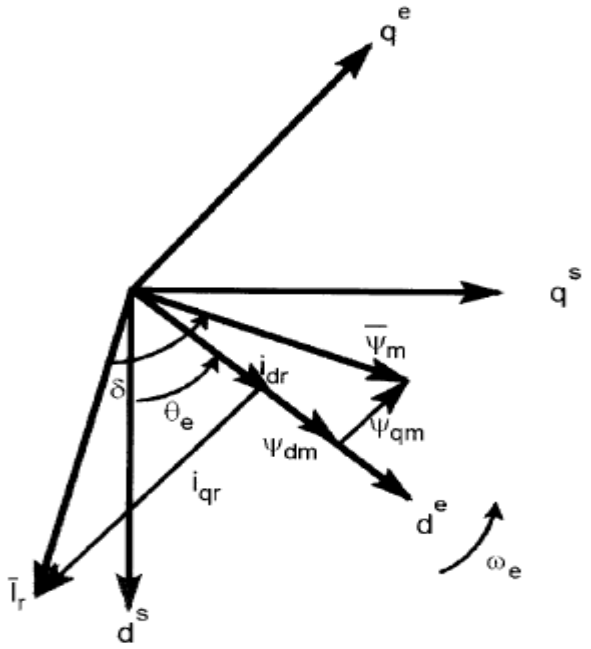

Figure 3.6 flux and current vectors in d^e-q^e frame (Bose, 2002)

Equations (3.27), (3.28) and (3.38) give the complete model of the electro-mechanical dynamics of an induction machine in synchronous frame. The composite system is of the fifth order and the nonlinearity of the model is evident. Figure 3.7 the

block diagram of the machine model along with input voltage and output current transformations (Bimal k bose, 2002).

3.3 (c) Stationary Frame-Dynamic Model

The dynamic machine in stationary frame can be derived simply substituting $\omega_e=0$ in equation (3.27) or in (3.15), (3.16), (3.19) and (3.20). The corresponding stationary frame equations are given as (Bose, 2002).

$$V_{qs}^{s} = R_s\, i_{qs}^{s} + d\psi_{qs}^{s}/dt \qquad (3.40)$$

$$V_{ds}^{s} = R_s\, i_{ds}^{s} + d\psi_{ds}^{s}/dt \qquad (3.41)$$

$$0 = R_r\, i_{qr}^{s} + d\psi_{qr}^{s}/dt - \omega_r\psi_{dr}^{s} \qquad (3.42)$$

$$0 = R_r\, i_{dr}^{s} + d\psi_{dr}^{s}/dt - \omega_r\psi_{qr}^{s} \qquad (3.43)$$

Where $v_{qr} = v_{dr} = 0$. Figure 3.8 shows the corresponding equivalent circuits. As mentioned before, in the stationary frame, the variables appear as sine waves in steady state with sinusoidal inputs. The torque equations (3.36) – (3.39) can also be written with the corresponding variables in stationary frame as (Bose, 2002).

$$T_e = (3/2)(p/2)\,(\psi_{dm}{}^{s}I_{qr}^{s} - \psi_{qm}{}^{s}I_{dr}^{s}) \qquad (3.44)$$

$$= (3/2)(p/2)\,(\psi_{dm}{}^{s}I_{qs}^{s} - \psi_{qm}{}^{s}I_{ds}^{s}) \qquad (3.45)$$

$$= (3/2)(p/2)\,(\psi_{ds}{}^{s}I_{qs}^{s} - \psi_{qs}{}^{s}I_{ds}^{s}) \qquad (3.46)$$

$$= (3/2)(p/2)L_m(i_{qs}{}^{s}i_{dr}^{s} - i_{ds}{}^{s}i_{qr}^{s}) \qquad (3.47)$$

$$= (3/2)(p/2)(\psi_{dr}{}^{s}I_{qr}^{s} - \psi_{qr}{}^{s}I_{dr}^{s}) \qquad (3.48)$$

Equations (3.13) – (3.14) and (3.42) – (3.43) can easily combined to drive the complex model as

$$V_{qds}^{s} = R_s i_{qds}^{s} + d\psi_{qds}^{s}/dt) \qquad (3.49)$$

$$0 = R_r\, i_{qds}^{s} + d\psi_{qdr}^{s}/dt - j\omega_r\psi_{qd} \qquad (3.50)$$

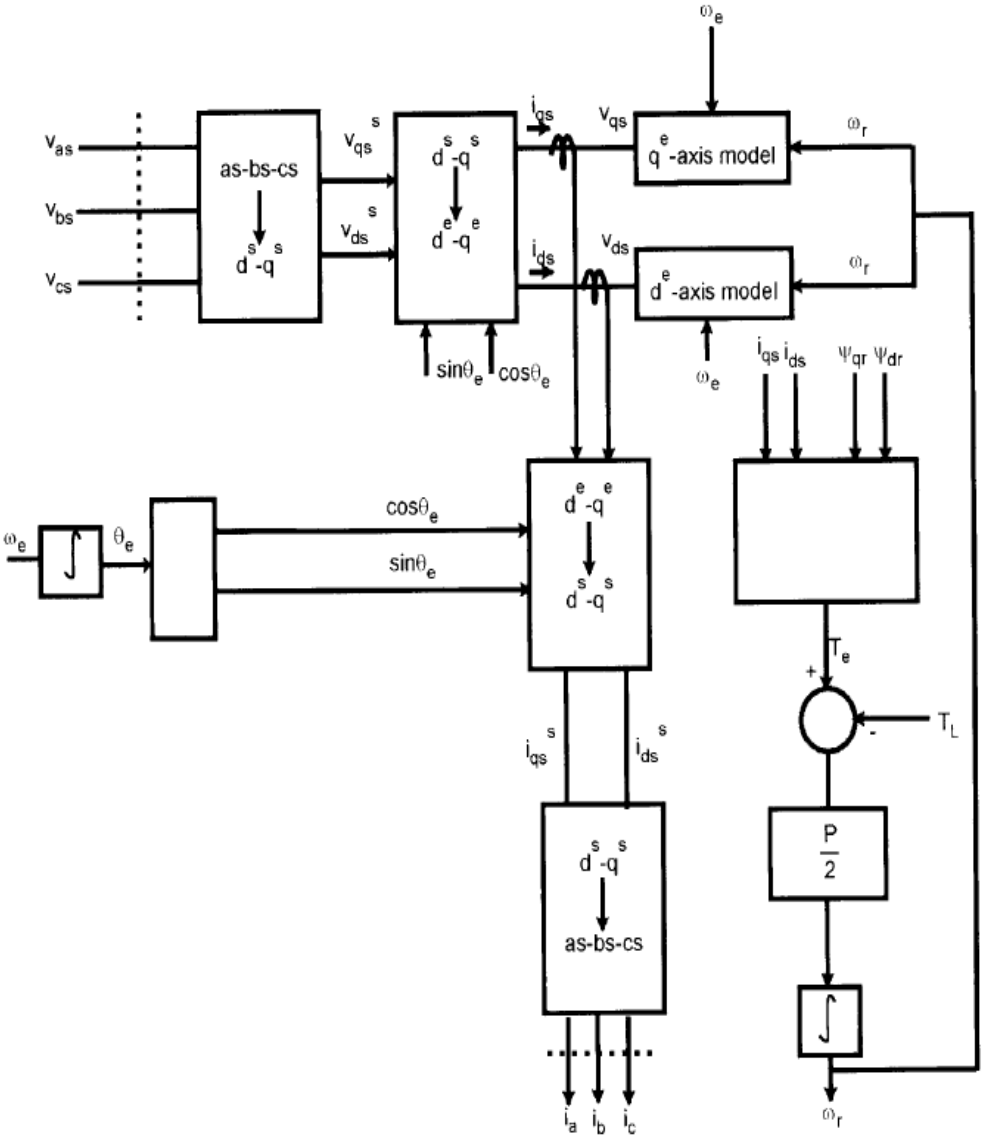

Figure 3.7 synchronously rotating frame machine model with input voltage and output current transformations (Bose, 2002)

Where $v_{qds}^{s} = v_{qs}^{s} - jv_{ds}^{s}$, $\psi_{qds}^{s} = \psi_{qs}^{s} - j\psi_{ds}^{s}$, $i_{qds}^{s} = i_{qs}^{s} - ji_{ds}^{s}$, $\psi_{qdr}^{s} = \psi_{qr}^{s} - j\psi_{dr}^{s}$, etc. The complex equivalent circuit in stationary frame is shown in figure 3.9(a). Often, per phase equivalent circuit with CEMF ($\omega_r\psi_r$) and sinusoidal variables is described in the form of figure 3.9(b) omitting the parameter L_m (Bose, 2002).

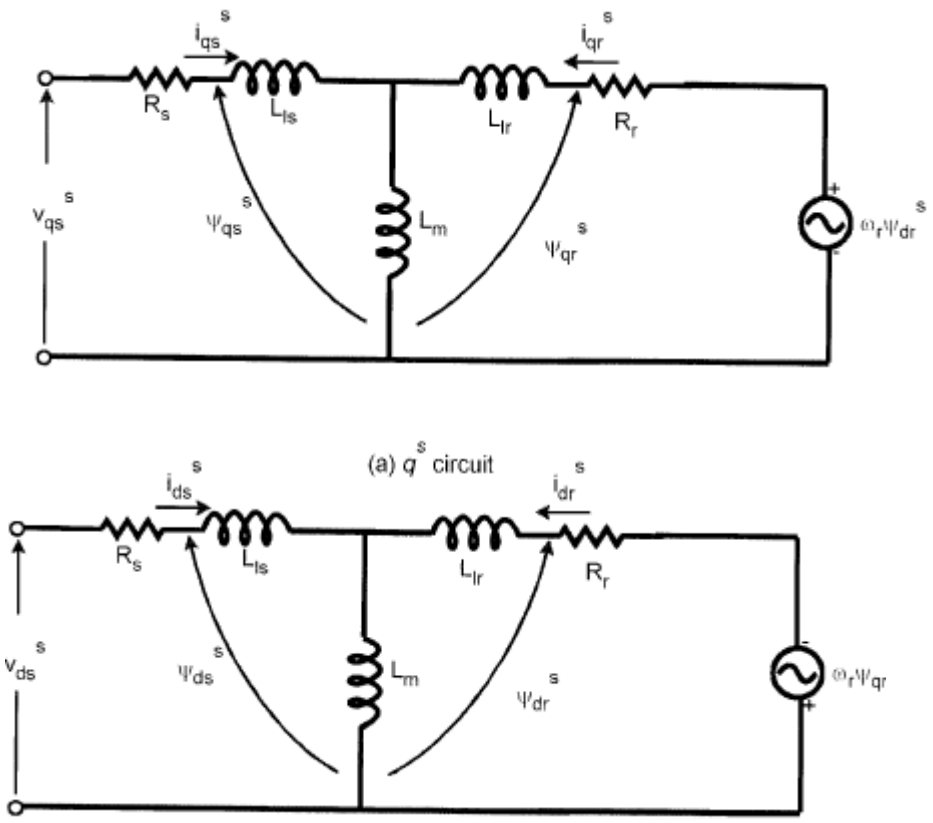

(b) ds ciruit

Fig 3.8 ds-qs equivalent circuits (Bose, 2002)

3.3 (d) Dynamic Model State-Space Equations

The dynamic machine model in state-space form is important for transient analysis, particularly for computer simulation study. Although the rotating frame model is generally preferred, the stationery frame model can also be used. The electrical variables in the model can be chosen as fluxes, currents, or a mixture of both. In this section, we will derive state-space equations of the machine in rotating frame with flux linkages as the main variables (Bose, 2002).

Let's define the flux linkage variables as follows:

$$F_{qs} = \omega_b \psi_{qs} \quad (3.51)$$

$$F_{qr} = \omega_b \psi_{qr} \quad (3.52)$$

$$F_{ds} = \omega_b \psi_{ds} \quad (3.53)$$

$$F_{dr} = \omega_b \psi_{dr} \quad (3.54)$$

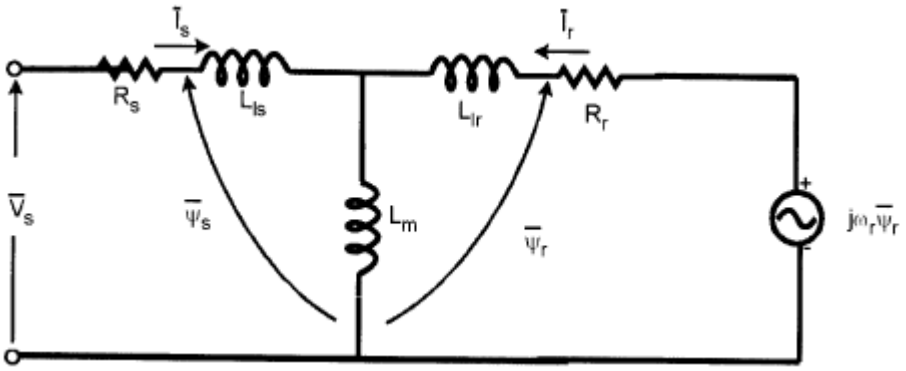

Figure 3.9(a) Stationary frame complex equivalent circuit (Bose, 2002)

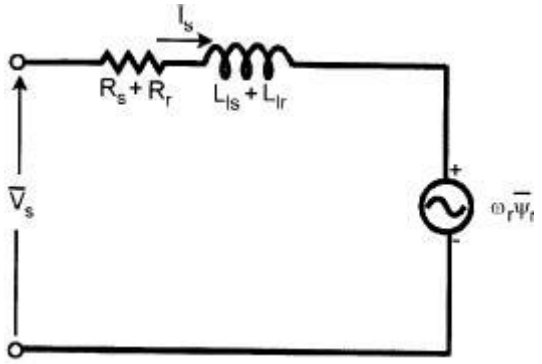

Figure 3.9 (b) Simplified per phase equivalent circuits (Bose, 2002)

Figure 3.9 Complex equivalent circuit with dqs equivalent circuits

Where ω_b = base frequency of the machine.

Substituting the above relations in equations (3.15), (3.16), (3.19) and (3.20), we can write

$$V_{qs} = R_s i_{qs} + (1/\omega_b)*dF_{qs}/dt + (\omega_e/\omega_b)F_{ds} \quad (3.55)$$

$$V_{ds} = R_s i_{ds} + (1/\omega_b)*dF_{ds}/dt - (\omega_e/\omega_b)F_{qs} \quad (3.56)$$

$$0 = R_r i_{qr} + (1/\omega_b)*dF_{qr}/dt + ((\omega_e - \omega_r)/\omega_b)F_{dr} \quad (3.57)$$

$$0 = R_r i_{dr} + (1/\omega_b)*dF_{dr}/dt - ((\omega_e - \omega_r)/\omega_b)F_{qr} \quad (3.58)$$

Where it is assumed that $v_{qr} = v_{dr} = 0$.

Multiplying equations (3.21) – (3.26) by ω_b on both sides, the flux linkage expressions can be written as

$$F_{qs} = \omega_b\psi_{qs} = X_{ls}i_{qs} + X_m(i_{qs} + i_{qr}) \quad (3.59)$$

$$F_{qr} = \omega_b\psi_{qr} = X_{lr}i_{qr} + X_m(i_{qs} + i_{qr}) \quad (3.60)$$

$$F_{qm} = \omega_b\psi_{qm} = X_m(i_{qs} + i_{qr}) \quad (3.61)$$

$$F_{ds} = \omega_b\psi_{ds} = X_{ls}i_{qs} + X_m(i_{ds} + i_{dr}) \quad (3.62)$$

$$F_{dr} = \omega_b\psi_{dr} = X_{lr}i_{qr} + X_m(i_{ds} + i_{dr}) \quad (3.63)$$

$$F_{dm} = \omega_b\psi_{dm} = X_m(i_{ds} + i_{dr}) \quad (3.64)$$

Where $X_{ls} = \omega_b l_{ls}$, $X_{lr} = \omega_b l_{lr}$, $X_m = \omega_b l_m$, or

$$F_{qs} = X_{ls}\, i_{qs} + F_{qm} \quad (3.65)$$

$$F_{qr} = X_{lr}\, i_{qr} + F_{qm} \quad (3.66)$$

$$F_{ds} = X_{ls}\, i_{ds} + F_{dm} \quad (3.67)$$

$$F_{dr} = X_{lr}\, i_{dr} + F_{dm} \quad (3.68)$$

From equations (3.65)-(3.68) the currents can be expressed in terms of the flux linkages as

$$I_{qs} = (F_{qs} - F_{qm})/X_{ls} \quad (3.69)$$

$$I_{qr} = (F_{qr} - F_{qm})/X_{lr} \quad (3.70)$$

$$I_{ds} = (F_{ds} - F_{dm})/X_{ls} \quad (3.71)$$

$$I_{dr} = (F_{dr} - F_{dm})/X_{ls} \quad (3.72)$$

Substituting equations (3.69)-(3.72) in (3.65)-(3.66) respectively, the F_{qm} expression is given as

$$F_{qm} = X_{ml}[((F_{qs} - F_{qm})/X_{ls}) + ((F_{qr} - F_{qm})/X_{lr})] \quad (3.73)$$

$$F_{qm} = (X_{ml}/X_{ls})F_{qs} + (X_{ml}/X_{lr})F_{qr} \quad (3.74)$$

Where

$$X_{ml} = 1/((1/X_m)+(1/X_{ls})+(1/X_{lr} \quad (3.75)$$

Similar derivation can be made for F_{qm} as follows:

$$F_{dm} = (X_{ml}/X_{ls})F_{ds} +(X_{ml}/X_{lr})F_{dr} \quad (3.76)$$

Substituting the current equations (3.69)-(3.72) into the voltage equations (33.55)-(33.68),

$$V_{qs} = R_s(F_{qs} – F_{qm})/ X_{ls} + (1/\omega_b)*dF_{qs}/dt + (\omega_e/\omega_b) \quad (3.77)$$

$$V_{ds} = R_s(F_{ds} – F_{dm})/ X_{ls} + (1/\omega_b)*dF_{ds}/dt - (\omega_e/\omega_b)F_{qs} \quad (3.78)$$

$$0 = R_r(F_{qr} – F_{qm})/ X_{lr} + (1/\omega_b)*dF_{qr}/dt + ((\omega_e – \omega_r) /\omega_b)F_{dr} \quad (3.79)$$

$$0 = R_s(F_{dr} – F_{dm})/ X_{lr} + (1/\omega_b)*dF_{dr}/dt - ((\omega_e – \omega_r) /\omega_b)F_{qr} \quad (3.80)$$

This can be expressed in state-space form as

$$dF_{qs}/dt = \omega_b[v_{qs} - (\omega_e/\omega_b)F_{ds} – (R_s/X_{ls}) (F_{qs} – F_{qm}) \quad (3.81)$$

$$dF_{ds}/dt = \omega_b[v_{qs} - (\omega_e/\omega_b)F_{qs} – (R_s/X_{ls}) (F_{ds} – F_{dm}) \quad (3.82)$$

$$dF_{qr}/dt = -\omega_b[((\omega_e – \omega_r)/\omega_b)F_{dr} – (R_r/X_{lr}) (F_{qr} – F_{qm})] \quad (3.83)$$

$$dF_{dr}/dt = -\omega_b[- ((\omega_e – \omega_r)/\omega_b)F_{qr} – (R_r/X_{lr}) (F_{dr} – F_{dm})] \quad (3.84)$$

Finally, from equation (3.37)

$$\mathbf{T_e = (3/2)(p/2) (F_{ds}i_{qs} – F_{qs}i_{ds})} \quad \mathbf{(3.85)}$$

Equations (3.81)-(3.85), along with Equation (3.28), describe the complete dynamic model in state-space form. F_{qs}, F_{ds}, F_{qr}, F_{dr} are the state variables (Bimal k bose, 2002).

Chapter 4 SIMULATION AND RESULTS

In the previous chapters we have discussed, the dynamic model of IM plant and the model were presented. In this chapter, using MATLAB-SIMULINK, simulations are performed to estimate the functional block such as torque, speed, flux, resistance WITH and WITHOUT fuzzy logic.

4.1 SIMULATION ENVIRONMENT

MATLAB-SIMULINK tools are used for model architecture development and simulations. This model is detailed enough that it can be used for evaluating the transient and steady-state response of the IM. Table 4.1 shows the technical specifications of the IM used for the plant model. The simulation circuits of functional block diagram i.e. Resistance estimator, Main circuit: DTC and Induction model are shown in figure 4.1 and 4.2. The membership functions and rules for the fuzzy duty ratio controller are shown in Fig. 4.3(a) (b) (c) (d). Stator flux estimator and the flux trajectories are obtained in the figure 4.4(a) (b) (c) (d). The surface viewer of quasi fuzzy logic is shown in the figure 4.5. Current and voltage waveforms can be obtained in the figure 4.6(a) (b) (c) and 4.7 (a) (b). Torque hysteresis, speed estimator have been developed as shown in figure 4.8 (a) (b) (c) 4.9 (a) (b) (c) (d) (e) (f). Voltage Source Inverter (VSI) is analyzed by using MATLAB S-function and is given in Software. The complete circuit model developed for DTC without fuzzy logic is shown in figure 4.10 in Chapter 3; a model of the induction machine controller that uses a fuzzy logic-based *d-q* control system to accurately control the dynamic response of the induction machine system is developed.

In order to have an accurate control of the induction machine, the flux linkage of the Induction machine must be known. It is, however, expensive and difficult to measure the flux. Instead, the flux can be estimated based on measurements of voltage, current and angular velocity, torque can be determined. Based on the reliability there are number of control strategies for the induction machine. Some prefer rotor flux, while others prefer stator. Throughout this chapter, it is assumed that the rotor current has different values i.e. it is working on no load and with load.

S No	Induction Machine Parameters	Predefined Values
1.	Stator Resistance(R_s)	2.7+R
2.	Rotor Resistance(R_r)	2.23
3.	Stator Inductance(L_s)	0.3562
4.	Rotor Inductance(L_r)	0.3362
5.	Mutual Inductance(L_m)	0.3425
6.	Friction Coefficient (J)	0.0025
7.	Number of poles (N)	2

Table 4.1 Simulation of DTC with and without Fuzzy Logic

4.2 Modeling of voltage source inverter (VSI)

The voltage source inverter is modeled in the form of *S-function block*, contained in voltage vector selection block. It is written in form of an S-function in the model, which gives the output of the inverter in terms of three phase voltages as per the signals received from optimum pulse selector. The S-function is given in Software. Overall model diagram of DTC realized is shown in Fig. 4.1.

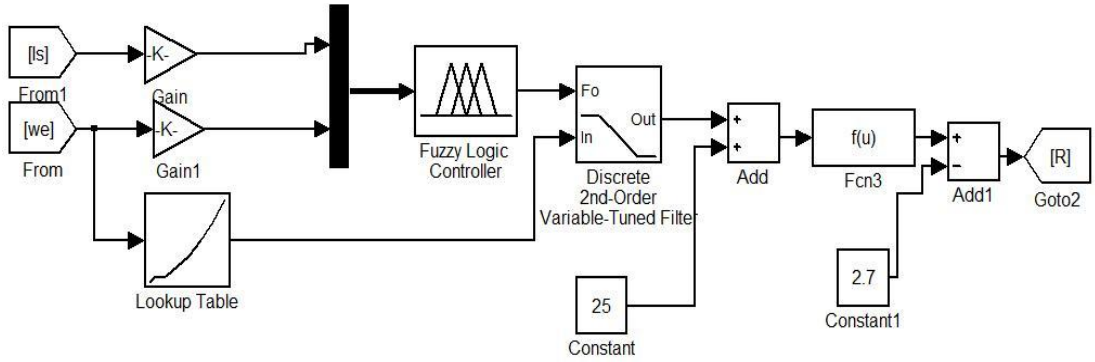

Figure 4.1 Estimator of Stator Resistance including temperature effect

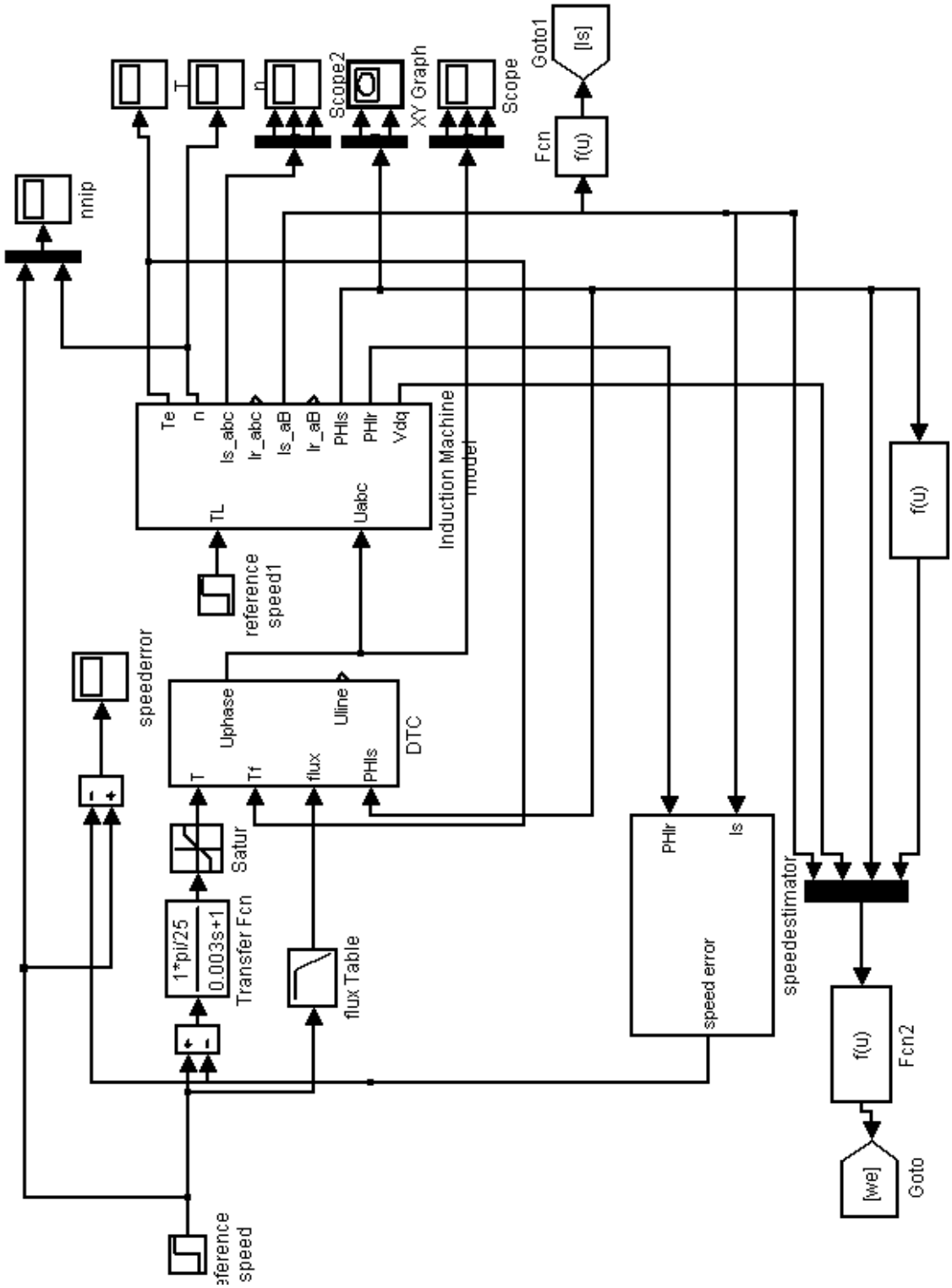

Figure 4.2 Main Circuit: DTC and Induction Motor model

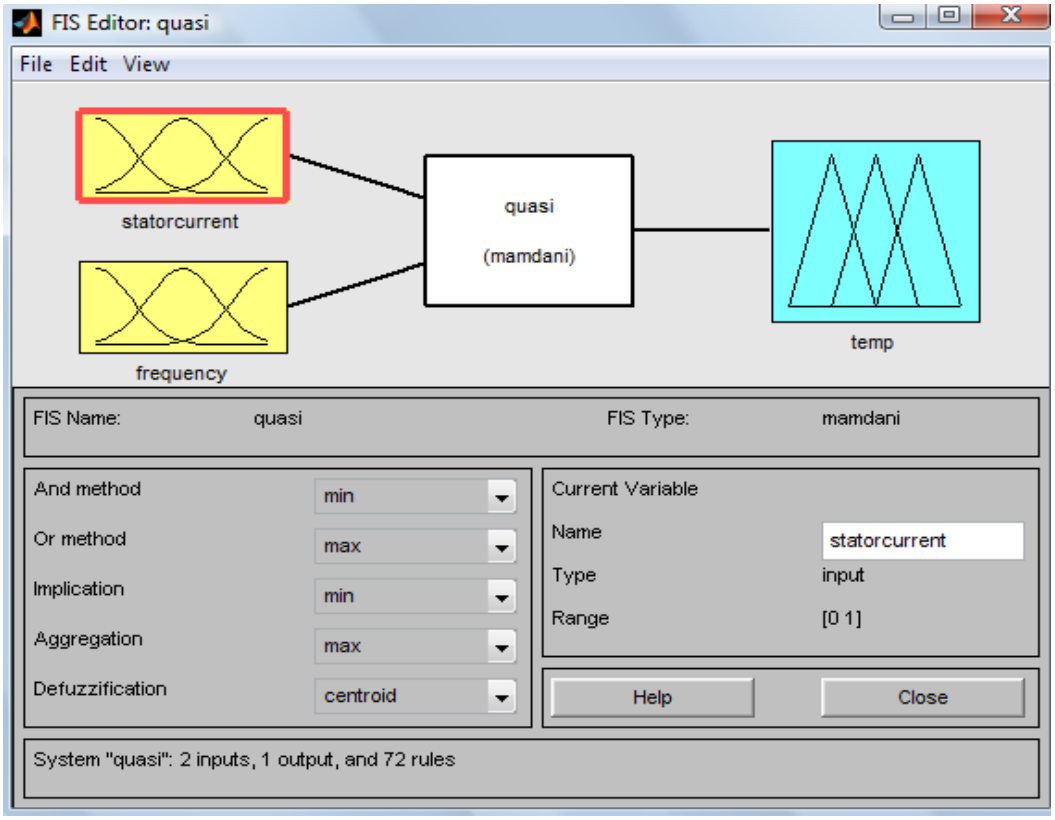

Figure 4.3 (a) FIS Editor

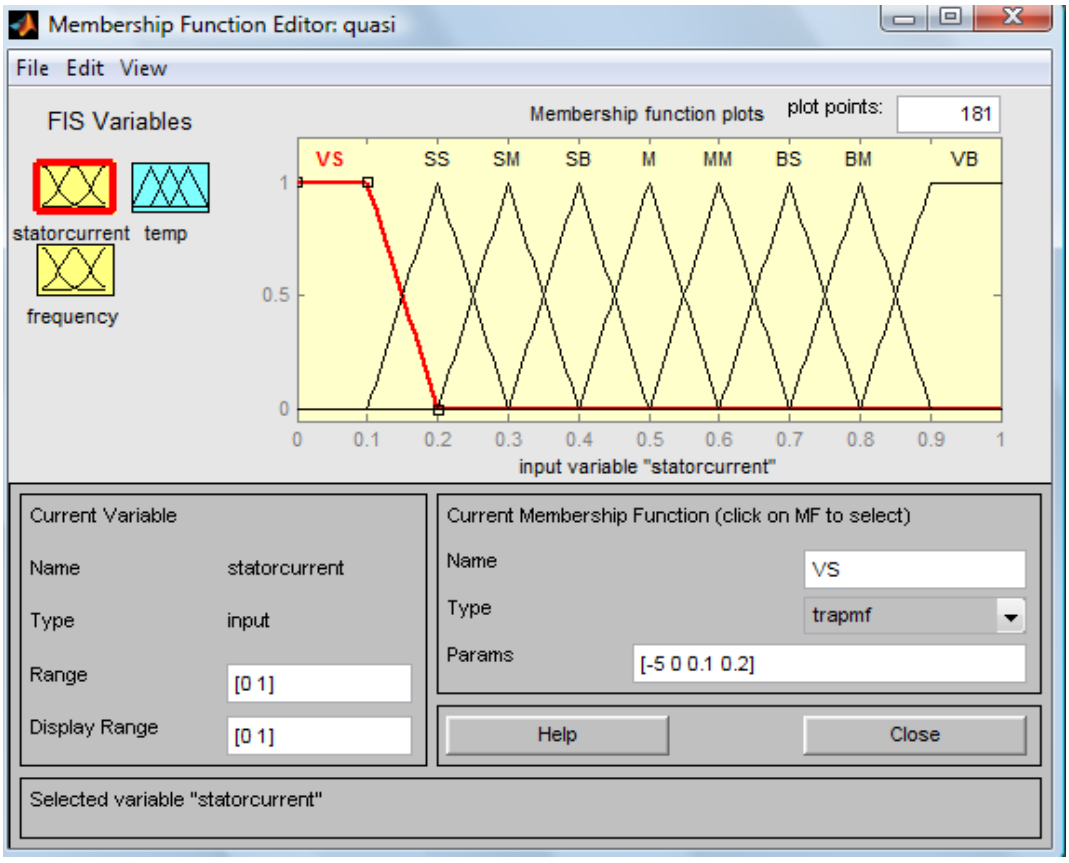

Figure 4.3 (b) Membership funcitions of stator current(Input1)

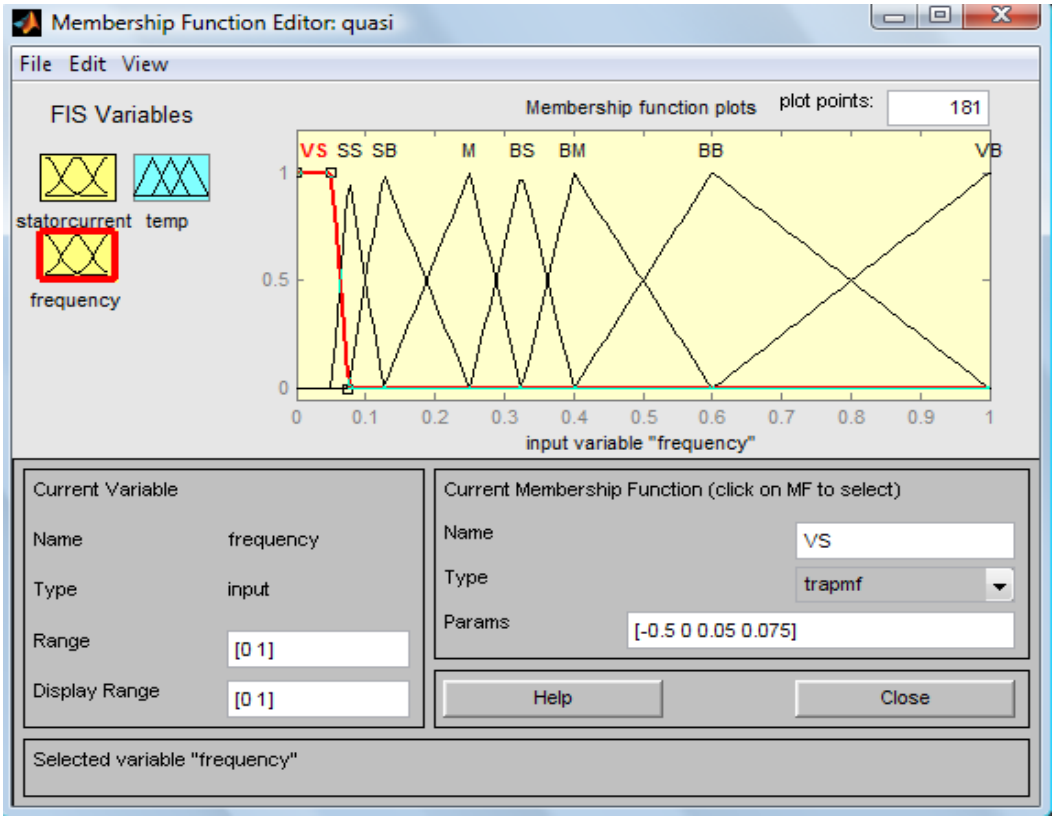

Figure 4.3(c) Membership functions of frequency (Input2)

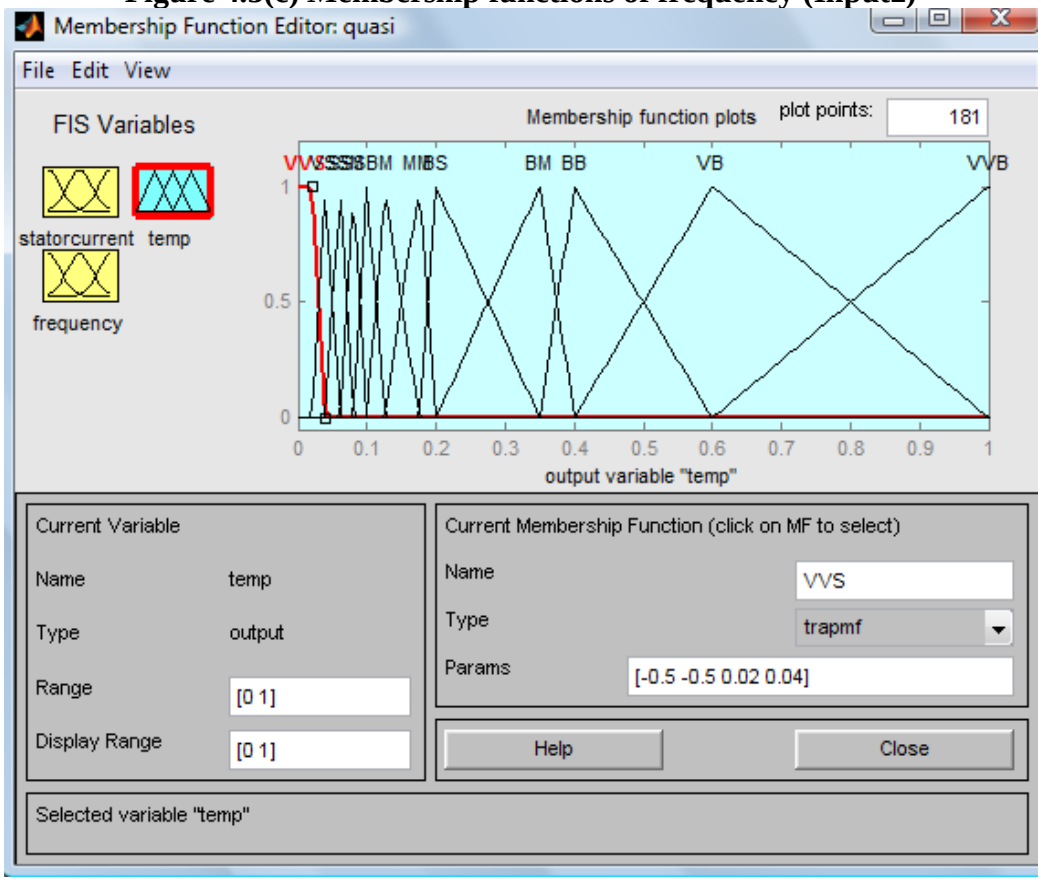

Figure 4.3(d) Membership functions of temperature (Output)

4.3 Modeling of functional Blocks

The DTC scheme uses flux and torque estimators to get the actual values at any instant. This is compared with the reference values to yield the error values which serve as the input to the voltage vector selection block. The modeling of various functional blocks of DTC is shown below:

4.3 (a) Estimator A Flux Model

Flux estimation is done using the equation

$$\psi_{s\_est} = \sqrt{\Psi_{ds}^{\ 2} + \Psi_{qs}^{\ 2}} \qquad (4.1)$$

The model of flux estimation block is shown in Fig. 4.4

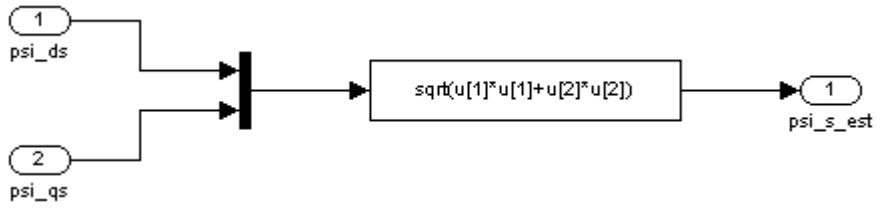

Figure 4.4 (a) Stator flux estimator

The development of Flux up to the reference value is shown in figure 4.4 (b), (c) and (d). With fuzzy logic duty ratio controller flux development is smooth. The reference value of the flux for the induction motor is taken as 0.9. The corresponding surface viewer for the fuzzy logic duty ratio controller is shown in figure 4.5 respectively.

4.3 (b) Estimator B Current model and Estimator C Voltage Model

Three phase currents are shown in Fig. 4.6 (a), (b) and (c) respectively for DTC without fuzzy logic, and with fuzzy logic and with load 0.9. It is very clear from the figures the current response is smooth when fuzzy logic applied.

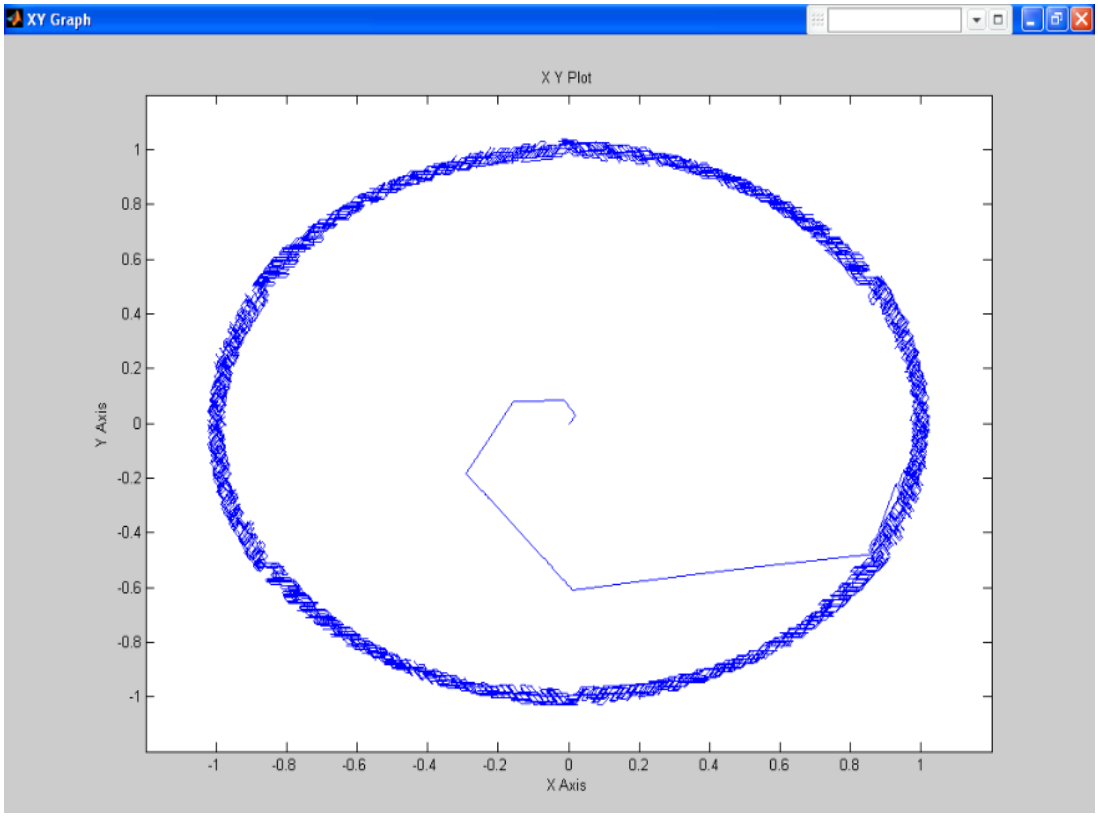

Figure 4.4 (b) Flux trajectory without fuzzy

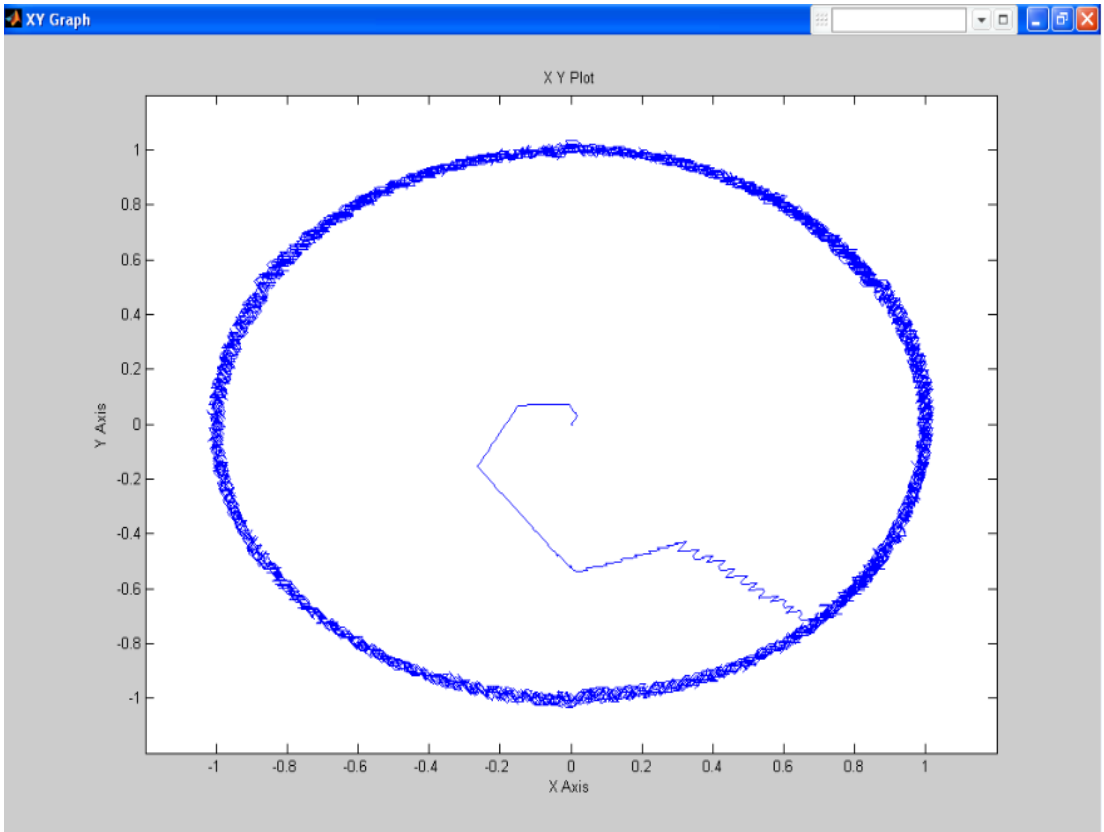

Figure 4.4 (c) Flux trajectory with fuzzy

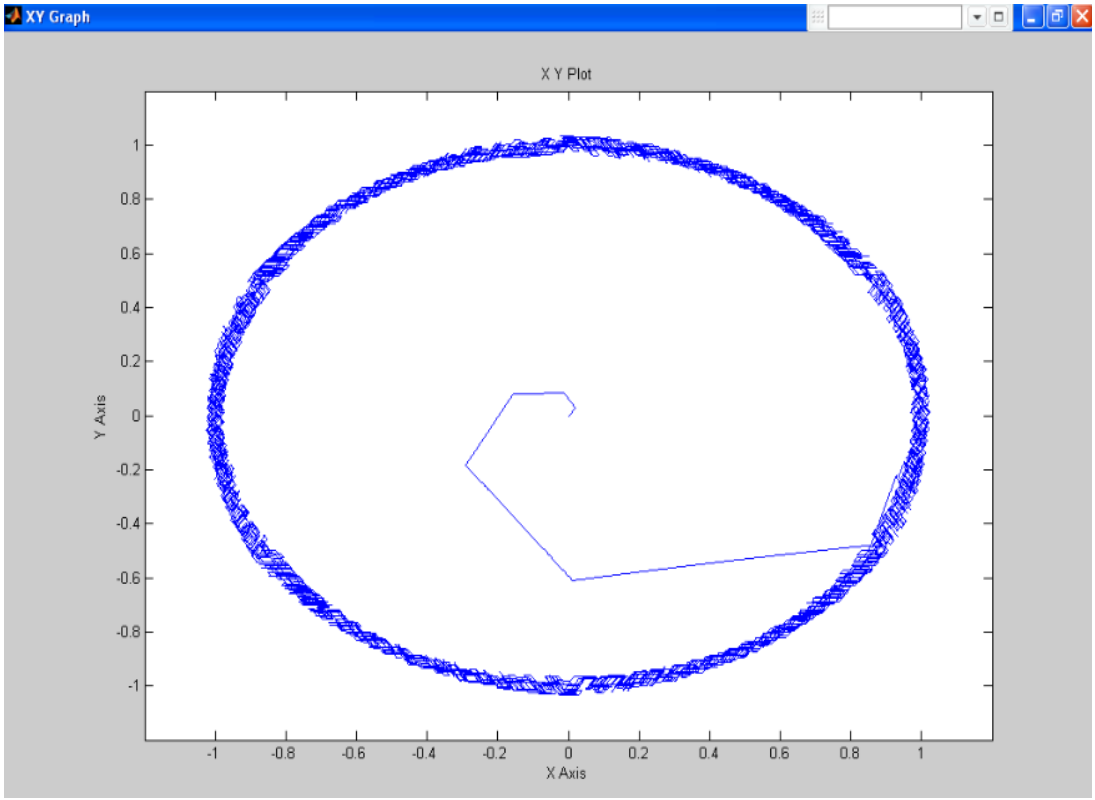

Figure 4.4 (d) Flux trajectory with load

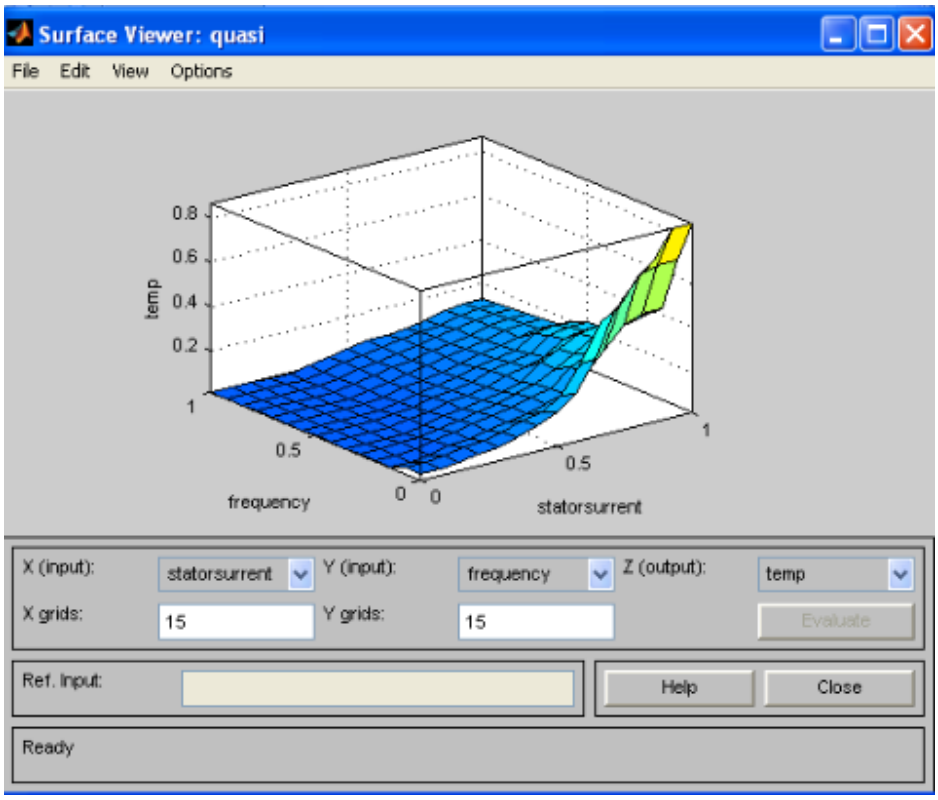

Figure 4.5 Surface viewer

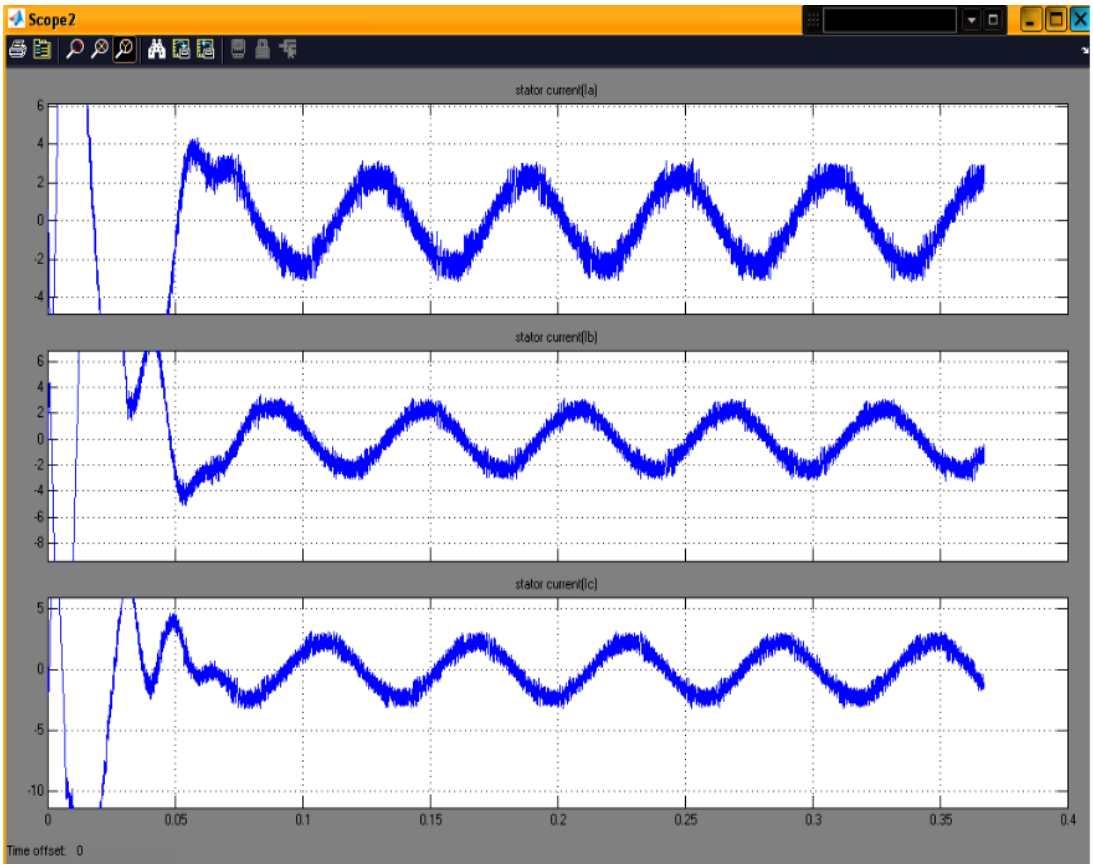

Figure 4.6(a) Stator current without fuzzy

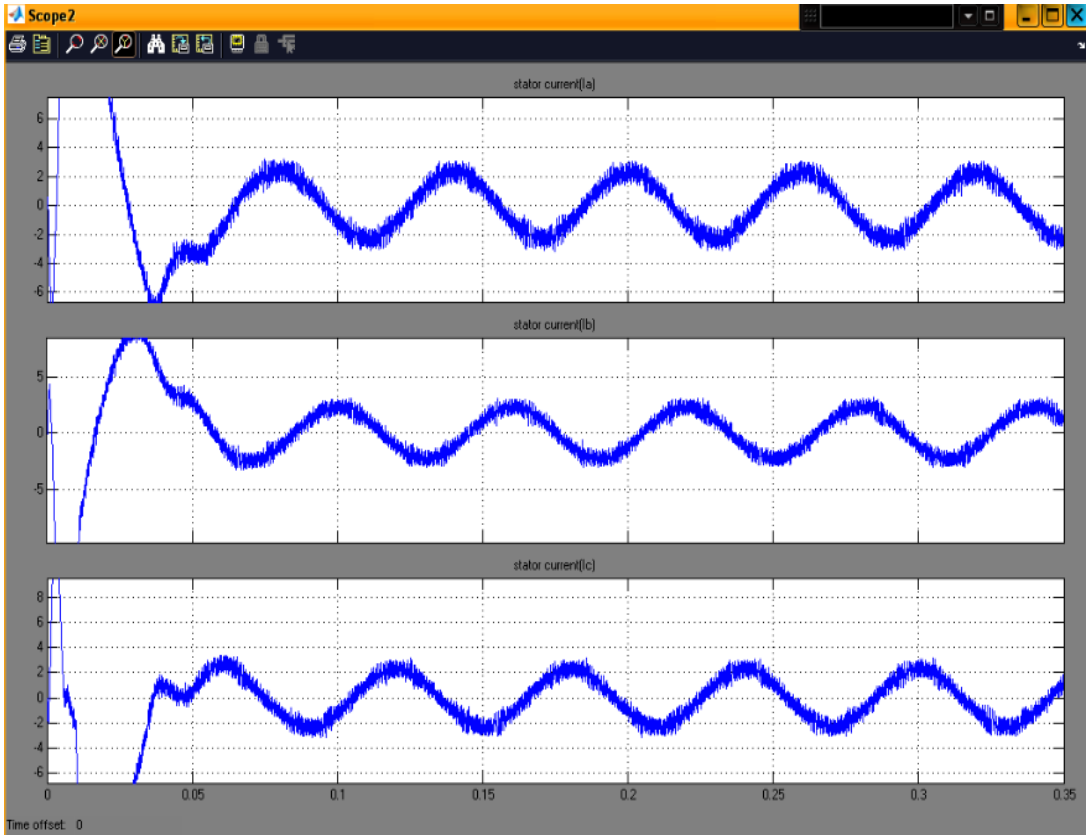

Figure 4.6 (b) Stator current with fuzzy

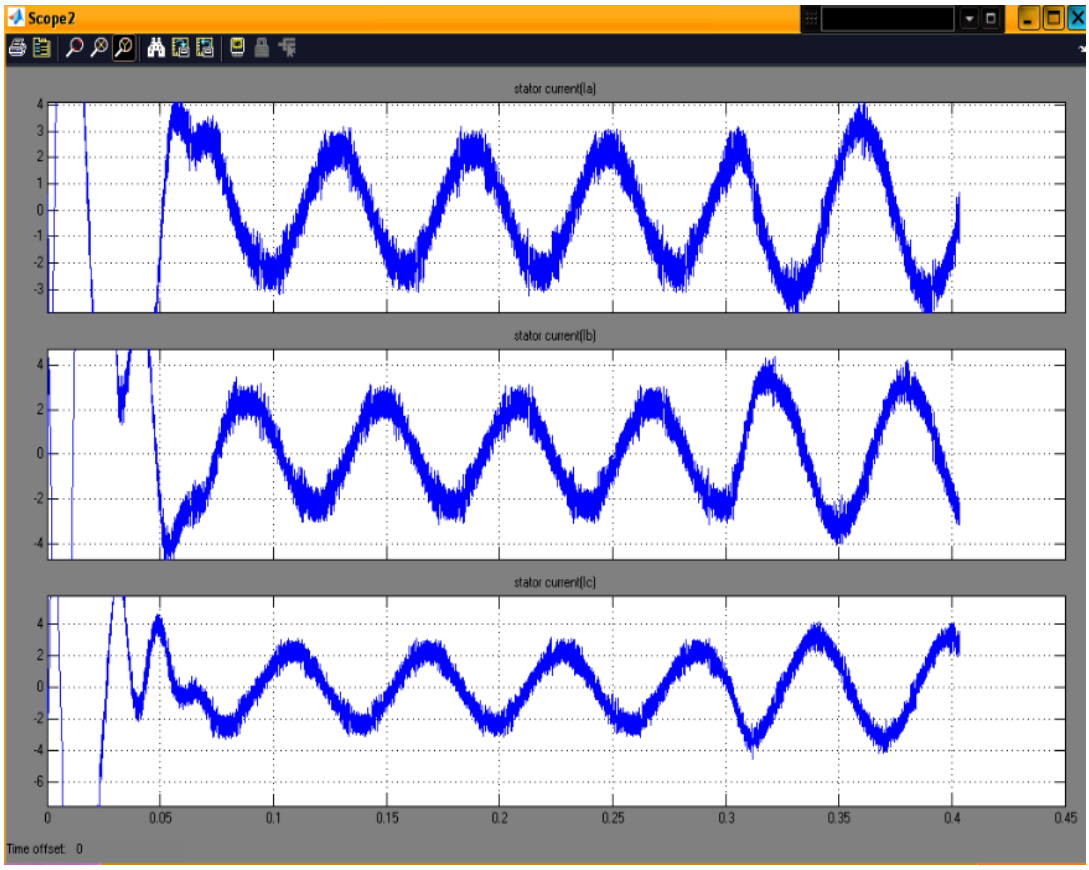

Figure 4.6 (c) Stator current with load

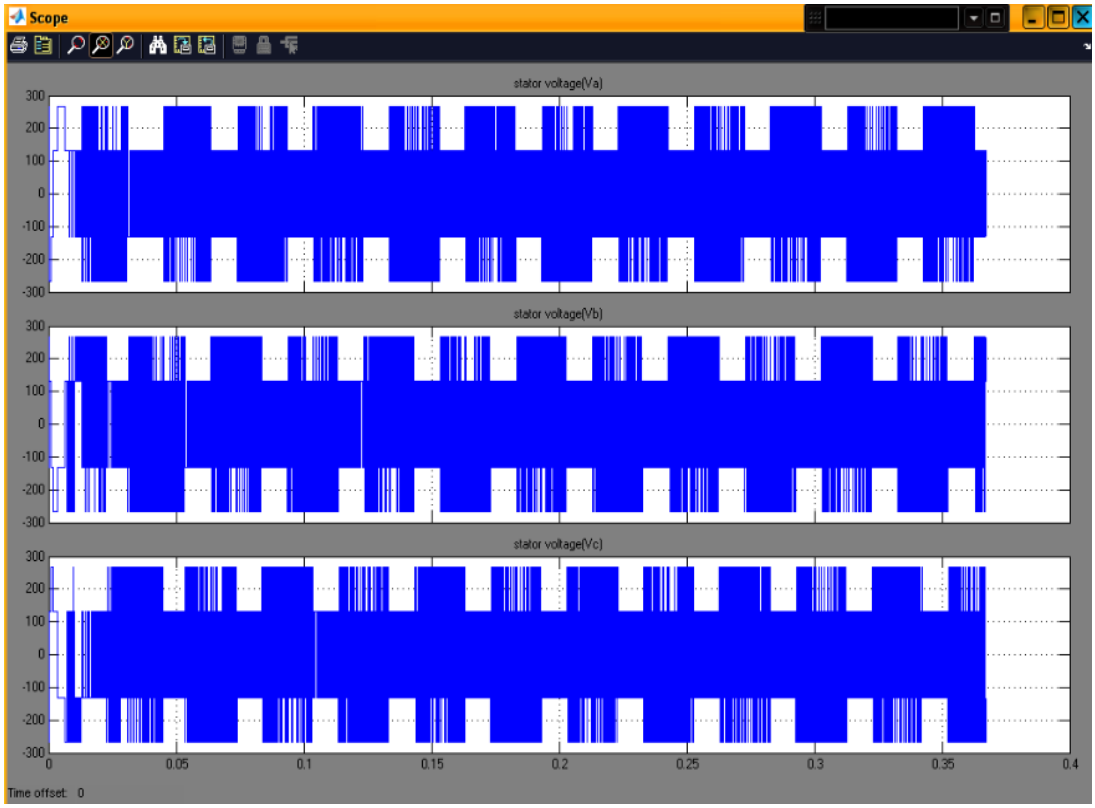

Figure 4.7 (a) Stator voltage without fuzzy

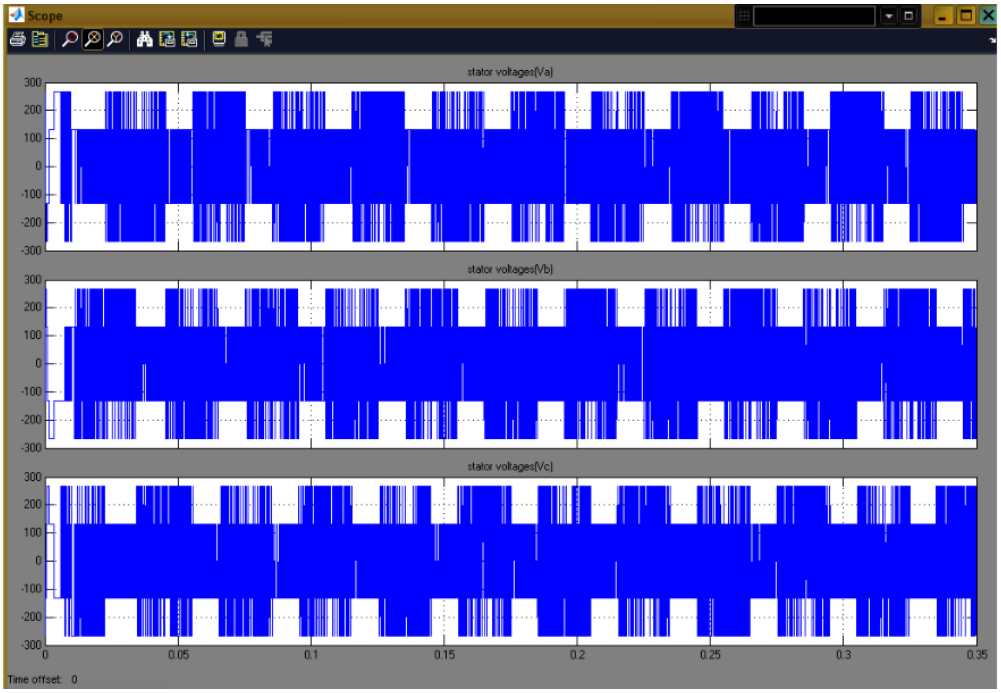

Figure 4.7 (b) Stator voltage with fuzzy

4.3 (b) Estimator D Torque and Speed Model

Torque estimation is done using following equation:

$$T_{est} = (3/2)\ (P/2)\ (\psi_{ds}\ i_{qs} - \psi_{qs}\ i_{ds}) \qquad (4.2)$$

The model of torque estimation block is shown at Fig. 4.5.

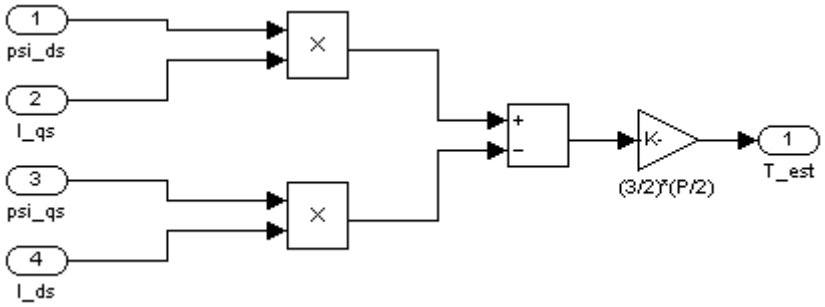

Figure 4.8(a) Torque Hysteresis

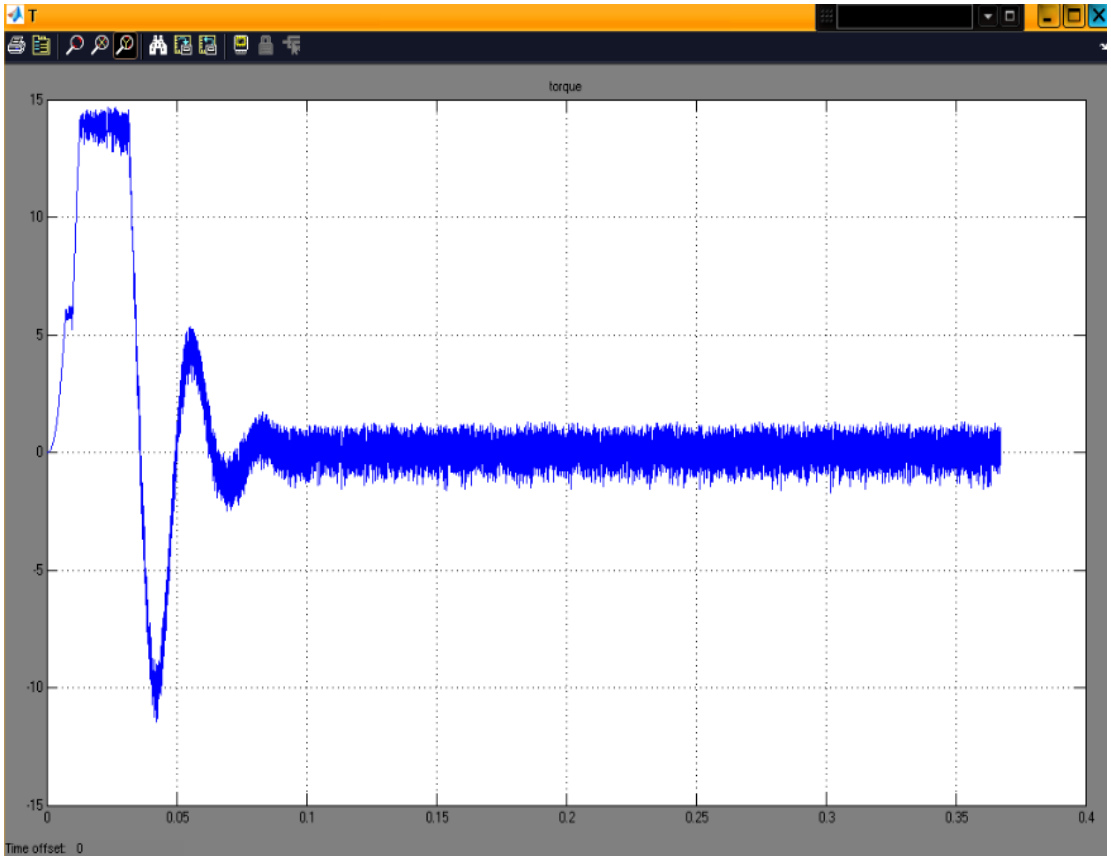

Figure 4.8 (b) Torque without fuzzy

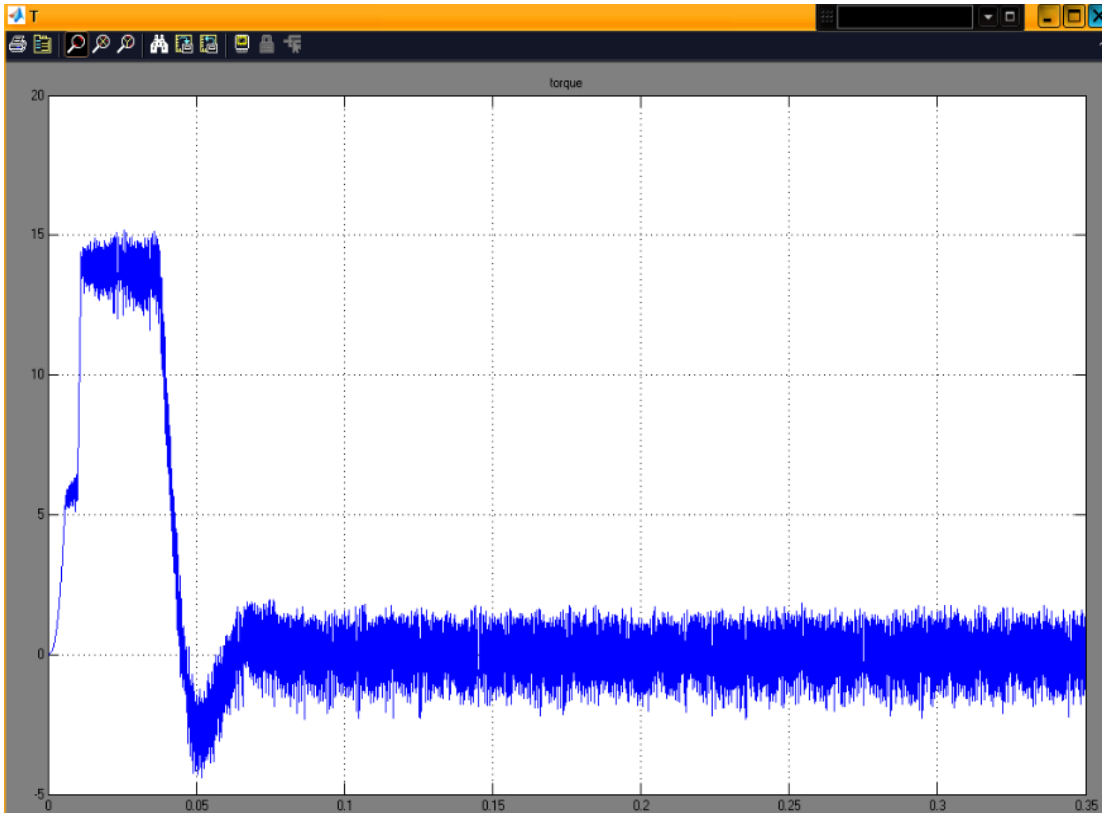

Figure 4.8 (c) Torque with fuzzy

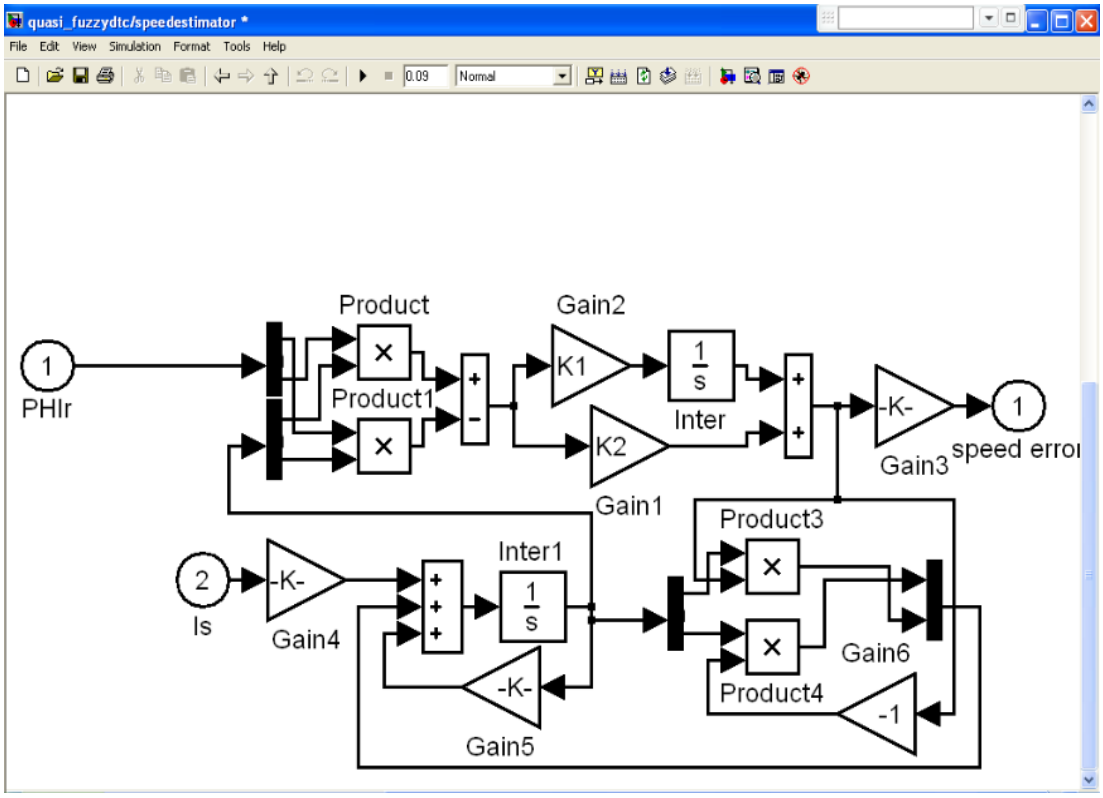

Figure 4.9 (a) Speed estimator

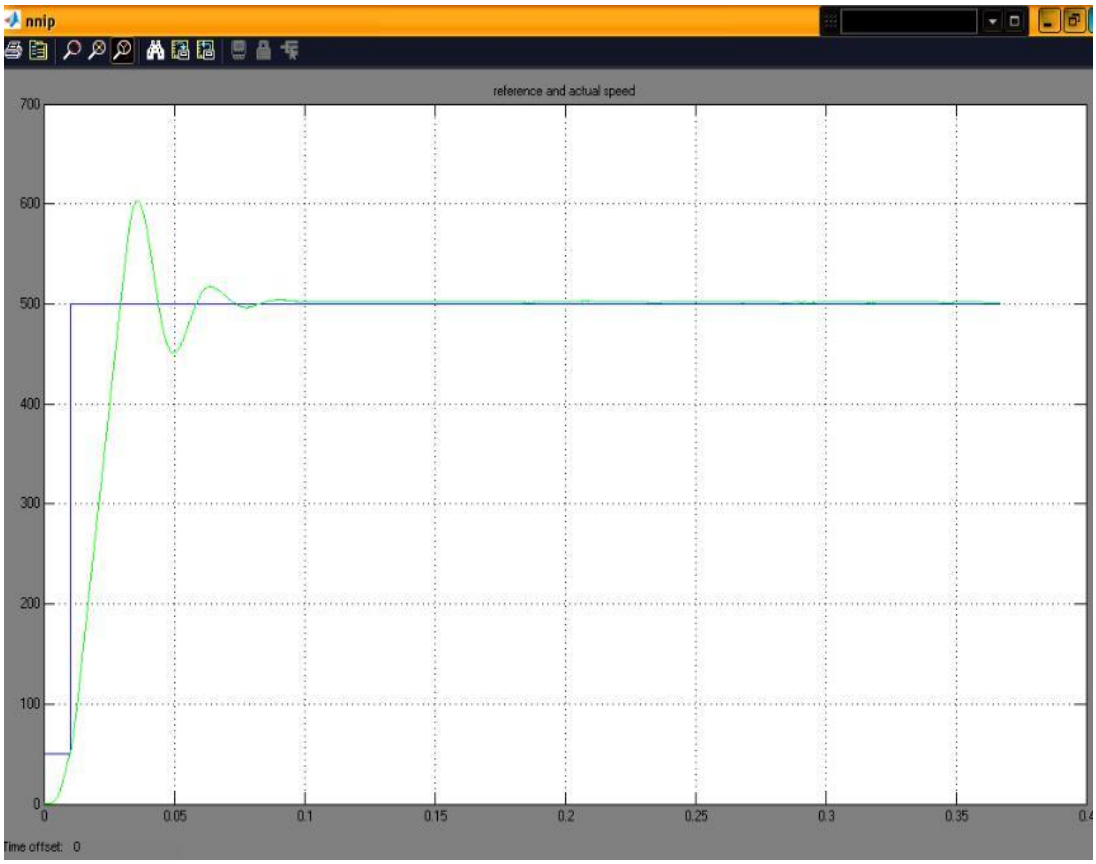

Figure 4.9(b) Speed and Reference without fuzzy

Figure 4.9 (c) Speed and Reference with fuzzy

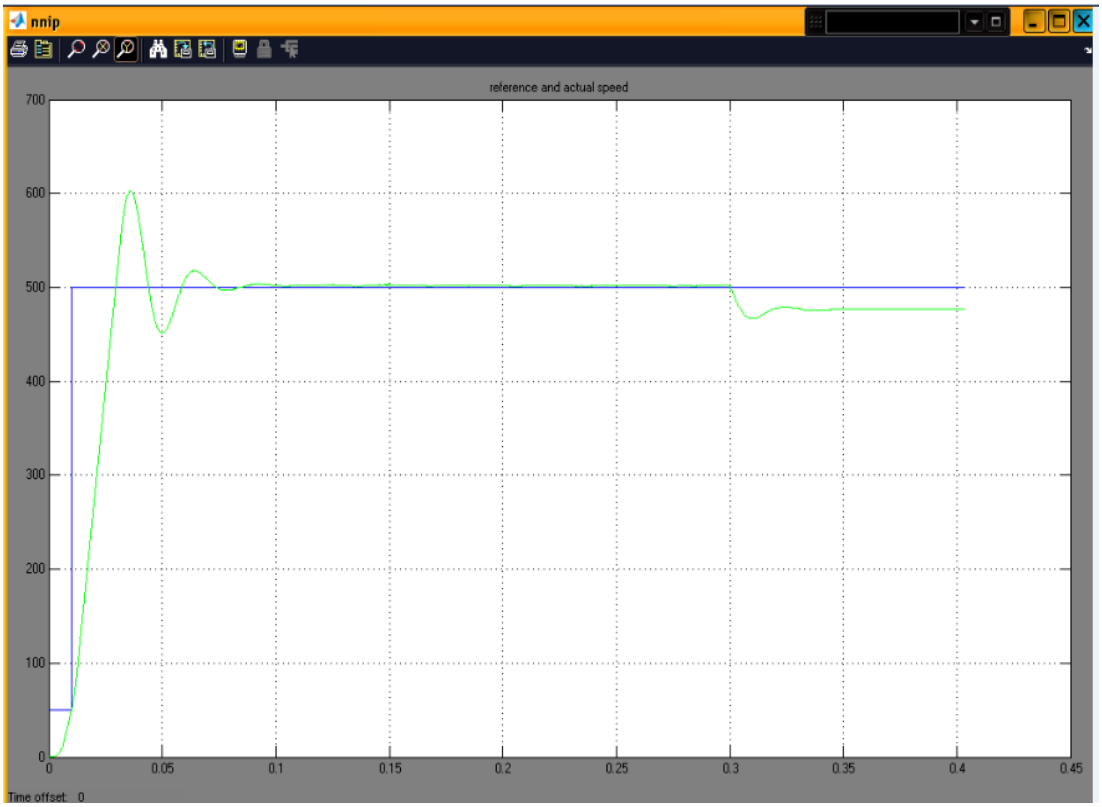

Figure 4.9 (d) Speed and Reference with load

Figure 4.9 (e) Speed Error without fuzzy

Figure 4.9(f) Speed Error with fuzzy

4.4 Modeling of Induction Motor in MATLAB-SIMULINK

The following assumptions are made for simplification:

1) The magnetic circuit of the machine is linear i.e. saturation effects are neglected.
2) The air gap of the machine is uniform and electromagnetic field is sinusoidally distributed i.e. the space harmonics and their effect on torque and induced voltages are neglected.
3) Parameters of machine remain constant.
4) The damping coefficients with mechanical system are neglected.

The equations of a 3-phase induction motor in stationary reference frame can be written as (Bose, 2002).

$$v_{qs} = R_s i_{qs} + p\psi_{qs} \quad (4.1)$$

$$v_{ds} = R_s i_{ds} + p\psi_{ds} \quad (4.2)$$

$$v_{qr} = R_r i_{qr} - \omega_r \psi_{dr} + p\psi_{qr} \quad (4.3)$$

$$v_{dr} = R_r i_{dr} + \omega_r \psi_{qr} + p\psi_{dr} \quad (4.4)$$

$$\psi_{qs} = (L_{ls} + L_m) i_{qs} + L_m i_{qr} \quad (4.5)$$

$$\psi_{ds} = (L_{ls} + L_m) i_{ds} + L_m i_{dr} \quad (4.6)$$

$$\psi_{qr} = L_m i_{qs} + (L_{lr} + L_m) i_{qr} \quad (4.7)$$

$$\psi_{dr} = L_m i_{ds} + (L_{lr} + L_m) i_{dr} \quad (4.8)$$

For a squirrel cage rotor induction motor, $v_{qr} = v_{dr} = 0$. The above equation on further simplification gives:

$$\psi_{qr} = i_{qs} (L_m R_r / (L_r.s + R_r)) + \psi_{dr} (L_r \omega_r / (L_r.s + R_r)) \quad (4.9)$$

$$\psi_{dr} = i_{ds} (L_m R_r / (L_r.s + R_r)) - \psi_{qr} (L_r \omega_r / (L_r.s + R_r)) \quad (4.10)$$

$$i_{ds} = v_{ds} (1/(L_{sm}.s + R_s)) - (\psi_{dr} / L_r) (L_m.s / (L_{sm}.s + R_s)) \quad (4.11)$$

$$i_{qs} = v_{qs} (1/(L_{sm}.s + R_s)) - (\psi_{qr} / L_r) (L_m.s / (L_{sm}.s + R_s) \quad (4.12)$$

Where, $L_s = L_{ls} + L_m$; $Lr = L_{lr} + L_m$ and $L_{sm} = L_m + L_{ls} - (L_m^2/L_r)$

Also, from equation 4.1 and 4.2,

$$\psi_{ds} = \int (v_{ds} - R_s i_{ds}) dt \quad (4.13)$$

$$\psi_{qs} = \int (v_{qs} - R_s i_{qs}) dt \quad (4.14)$$

For electromagnetic torque calculation, the following equations are used:

$$T_{em} = (3/2)(P/2)\,(L_m/L_r)\,(\psi_{dr}\, i_{qs} - \psi_{qr}\, i_{ds}) \quad (4.15)$$

$$T_{em} - T_{load} = J\,(d\omega_r / dt) \quad (4.16)$$

The induction motor has been modeled using equations (4.9) to (4.16).

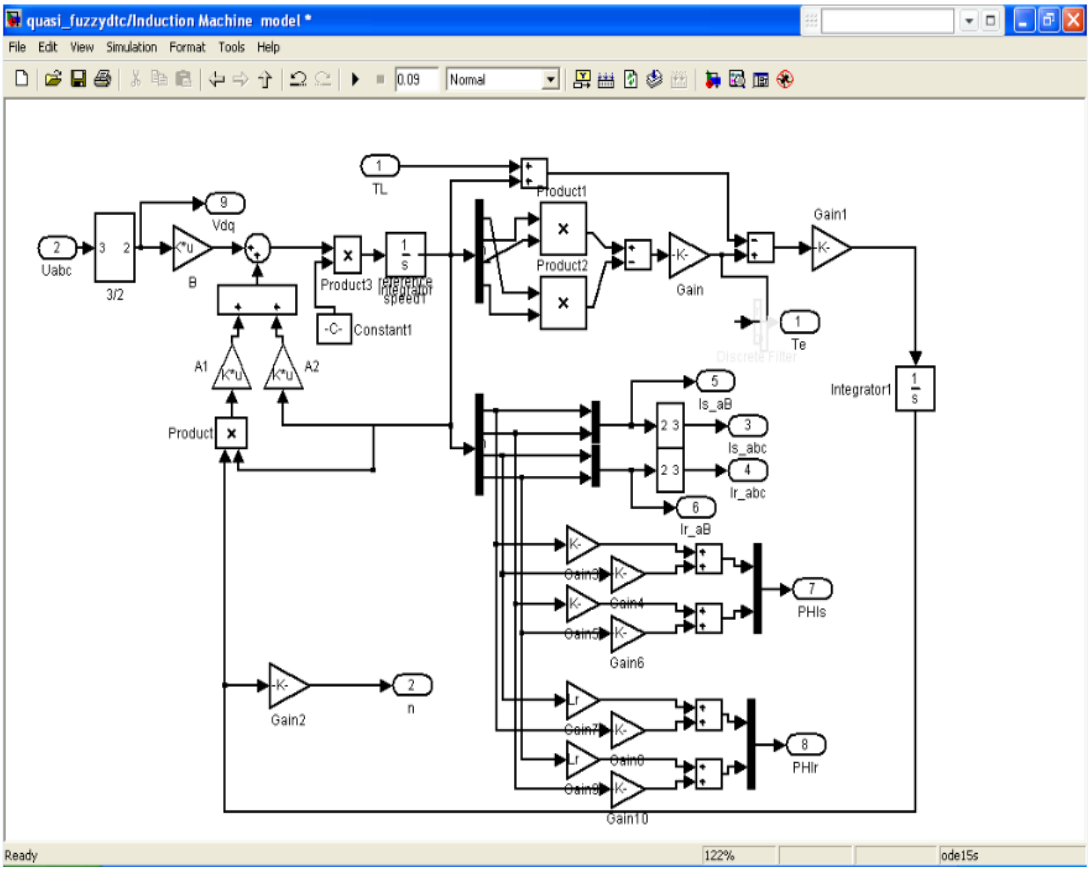

Figure 4.10 Induction motor model

Chapter 5 Conclusion

The estimation of rotor flux of an induction is measured indirectly. Direct torque and flux control was introduced for voltage fed PWM inverters. In the recent year major companies are showing interest and one of them introduced a scheme which is used to control the flux and torque. The scheme is to control the torque and stator flux of drive independently by inverter voltage space vector selection through a lookup table.

As we discuss earlier there are many ways to estimate the modelling functional blocks of the IM. . Fuzzy logic application in electronic industry is new. The applications demonstrated the superiority of the fuzzy systems to the conventional control systems.

The main aim behind this work was to develop a Dynamic model for estimation of functional blocks in MATLAB. After the implementation it was observed that the torque is having more ripples. Then while searching the methods to improve the performance it was found in the literature the duty ratio controller for the switched reluctance motor was implemented. So it was thought that the duty ratio controller may improve the performance. The duty ratio controller using fuzzy logic was implemented.

The models are developed for DTC without and with Fuzzy Logic in MATLAB/ SIMULINK and simulated.

The simulation results show the validation of Fuzzy Logic based DTFC method in achieving considerable reduction in torque ripple.

Future Direction

This work may be extended to implement Artificial Neural Networks (ANN), Neuro-Fuzzy system, Fuzzy –Genetic algorithms for the optimization of the scheme. The matrix converter to achieve DTC can be incorporated.

References

ALONGE, F. and D'IPPOLITO, F., (2007). "Design and sensitivity analysis of a reduced-order rotor flux optimal observer for induction motor control". *Control Engineering Practice,* **15**(12), pp. 1508-1519.

AMIN, B., (2002) *Induction motors: analysis and torque control,* Springer Verlag.

BARTOLO, J.B., STAINES, C.S. and CARUANA, C., (2008). "Flux position estimation using current derivatives for the sensorless control of AC machines", 2008, pp1468-1473.

BLAABJERG, F., TEODORESCU, R., ZELECHOWSKI, M., LACH, P. and ROZANSKI, P., (2005). "Rotor flux and speed estimators for induction motor drives". A performance evaluation, 2005.

BOSE, B. K., (2002), *Modern Power Electronics and AC Drives,* Prentice Hall PTR.

BOSE, B.K., and PATEL, N.R., (1998) "Quasi-fuzzy estimation of stator resistance of induction motor", *IEEE Transaction on Power Electronics,* **13**(3).

BOLDEA, I. and NASAR, S.A. (2001) *The Induction Machine handbook,* 1st ed., CRC press.

BUSAWON, K., YAHOUI, H., HAMMOURI, A. and GRELLET, G., (2001). "A nonlinear observer for induction motors". *EPJ Applied Physics,* **15**(3), pp. 181-188.

CARUANA, C., ASHER, G.M., BRADLEY, K.J. and WOOLFSON, M., (2003). "Flux position estimation in cage induction machines using synchronous HF injection and Kalman filtering". *IEEE Transactions on Industry Applications,* **39**(5), pp. 1372-1378.

GUERGAZI, A., MOUSSI, A. and DEBILOU, A., (2007). "Application of EKF algorithm for rotor speed, flux and resistance estimation in induction motors". *Modelling, Measurement and Control A,* **80**(1-2), pp. 28-37.

HAKIKI, K., MAZARI, B. and DJABER, S.A., (2007). "Induction motor flux estimation using nonlinear sliding observers". *Journal of Mathematics and Statistics,* **3**(2), pp. 65-69.

HEMSAS, K.E., OUHROUCHE, M., KHENFER, N. and LEULMI, S., (2005). "Estimation of speed, rotor resistance and rotor flux of an induction motor using neural networks and neuro-fuzzy techniques". *WSEAS Transactions on Computers,* **4**(6), pp. 637-642.

HENNEBERGER, H.C.G., (2002) Electric machines I Basic, Design, Function, Operation, Aachen University

HILAIRET, M., AUGER, F., BERTHELOT, E., (2009). "Speed and rotor flux estimation of induction machines using a two-stage extended Kalman filter", *Automatica,*

HOLTZ, J., and QUAN, J., (2003), "Drift and parameter compensated flux estimator for persistent zero stator frequency operation of sensorless controlled induction motor", **39**,4, 1052-1060.

HUMPHRIES, J.T., (1998) *Motors and Controls,* Columbus, Ohio: Merrill Publishing Company.

JIN, H., HUANG, J. and YANG, J.-., (2006). "Adaptive rotor flux estimation and parameter identification for induction motor". *Zhejiang Daxue Xuebao (Gongxue Ban)/Journal of Zhejiang University (Engineering Science),* **40**(2), pp. 339-343+351.

KOUZ, K., NART-SARCF, M.-., HILAIRE, M. and BERTHLO, E., 2009. A robust fuzzy speed estimation for vector control of an induction motor, 2009.

LIAN, K.-. and HUNG, C.-., (2006). "Sensorless control for induction motors via fuzzy observer design", 2006, pp2140-2145.

MEDVEDEV, A. and ZELL, C., (1994). "Designing a flux observer for induction machines", 1994, pp453-458

MENDRELA, E., FLESZAR, J., GIERCZAK, E., (2003) *Modeling of induction motors with one and two degrees of mechanical freedom* Kluwer Academic Publishers.

MACEK-KAMINSKA, K. and WACH, P., (1996). "Estimation of the parameters of mathematical models of squirrel-cage inductions motors", 1996, pp337-342.

ORLOWSKA-KOWALSKA, T., DYBKOWSKI, M. and SZABAT, K., 2007. Adaptive neuro-fuzzy control of the sensorless induction motor drive system, 2007, pp1836-1841.

ROBYNS, B., BUYSE, H. and LABRIQUE, F., 1998. Fuzzy logic based field orientation in an indirect FOC strategy of an induction actuator. *Mathematics and Computers in Simulation,* **46**(3-4), 265-274.

REHMAN, H. and DHAOUADI, R., (2008) "A fuzzy learning—Sliding mode controller for direct field-oriented induction machines", *Neurocomputing,* **71**(13-15), 2693-2701.

SAKAE, Y. (1986) *AC Motors for High-performance Applications Analysis and control*, New York: Dekker

STEPHEN, J.B. (2005) *Electric Machinery Fundamentals*, 4th ed., New York: Elizabeth A. Jones.

SUN, J., QIU, A. and SHI, W., (1999). "Rotor flux estimation of an induction motor using artificial neural networks". *Cailiao Yanjiu Xuebao/Chinese Journal of Materials Research,* **13**(1), pp. 1-3. F

TA-CAO, M. and LE-HUY, H., 1996. Model reference adaptive fuzzy controller and fuzzy estimator for high performance induction motor drives, 1996, pp380-387.

TRZYNADLOWSKI, A. M., (2001) *Control of Induction motors,* Academic press.

WANG, G., XU, D., YU, Y. and CHEN, W., (2008). "Improved rotor flux estimation based on voltage model for sensorless field-oriented controlled induction motor drives", 2008, pp1887-1890.

Walter, N.A. Jeff, K. (2001) *AC/DC Motors, Controls, and Maintenance,* 7th ed., USA: Cengage Learning.

ZHANG, C.-., LIN, F., SONG, W.-., GAO, L. and CHEN, S.-., (2003). "Rotor flux estimator of induction motor based on stator current vector orientation". *Zhongguo Dianji Gongcheng Xuebao/Proceedings of the Chinese Society of Electrical Engineering,* **23**(8), pp. 155-158.

ZHANG, H. and DAI, X., (2008). "Induction motor flux estimation based on Artificial Neural Network left-inversion", 2008, pp639-643.

ZHENG, Y. and LOPARO, K.A., (1999). "Adaptive flux and speed estimation for induction motors", 1999, pp25

Appendix A

[System]

Name='quasi'

Type='mamdani'

Version=2.0

NumInputs=2

NumOutputs=1

NumRules=72

AndMethod='min'

OrMethod='max'

ImpMethod='min'

AggMethod='max'

DefuzzMethod='centroid'

[Input1]

Name='statorcurrent'

Range=[0 1]

NumMFs=9

MF1='VS':'trapmf',[-5 0 0.1 0.2]

MF2='SS':'trimf',[0.1 0.2 0.3]

MF3='SM':'trimf',[0.2 0.3 0.4]

MF4='SB':'trimf',[0.3 0.4 0.5]

MF5='M':'trimf',[0.4 0.5 0.6]

MF6='MM':'trimf',[0.5 0.6 0.7]

MF7='BS':'trimf',[0.6 0.7 0.8]

MF8='BM':'trimf',[0.7 0.8 0.9]

MF9='VB':'trapmf',[0.8 0.9 1 1.5]

[Input2]

Name='frequency'

Range=[0 1]

NumMFs=8

MF1='VS':'trapmf',[-0.5 0 0.05 0.075]

MF2='SS':'trimf',[0.05 0.075 0.125]

MF3='SB':'trimf',[0.075 0.125 0.25]

MF4='M':'trimf',[0.125 0.25 0.325]

MF5='BS':'trimf',[0.25 0.325 0.4]

MF6='BM':'trimf',[0.325 0.4 0.6]

MF7='BB':'trimf',[0.4 0.6 1]

MF8='VB':'trapmf',[0.6 1 1.5 1.5]

[Output1]

Name='temp'

Range=[0 1]

NumMFs=12

MF1='VVS':'trapmf',[-0.5 -0.5 0.02 0.04]

MF2='VS':'trimf',[0.02 0.04 0.06]

MF3='SS':'trimf',[0.04 0.06 0.08]

MF4='SM':'trimf',[0.06 0.08 0.1]

MF5='SB':'trimf',[0.08 0.1 0.125]

MF6='M':'trimf',[0.1 0.125 0.175]

MF7='MM':'trimf',[0.125 0.175 0.2]

MF8='BS':'trimf',[0.175 0.2 0.35]

MF9='BM':'trimf',[0.2 0.35 0.4]

MF10='BB':'trimf',[0.35 0.4 0.6]

MF11='VB':'trimf',[0.4 0.6 1]

MF12='VVB':'trapmf',[0.6 1 1.5 1.5]

[Rules]

1 1, 2 (1) : 1

1 2, 2 (1) : 1

1 3, 1 (1) : 1

1 4, 1 (1) : 1

1 5, 1 (1) : 1

1 6, 1 (1) : 1

1 7, 1 (1) : 1

1 8, 1 (1) : 1

2 1, 3 (1) : 1

2 2, 3 (1) : 1

2 3, 2 (1) : 1

2 4, 2 (1) : 1

2 5, 1 (1) : 1

2 6, 1 (1) : 1

2 7, 1 (1) : 1

2 8, 1 (1) : 1

3 1, 4 (1) : 1

3 2, 4 (1) : 1

3 3, 3 (1) : 1

3 4, 3 (1) : 1

3 5, 2 (1) : 1

3 6, 2 (1) : 1

3 7, 1 (1) : 1

3 8, 1 (1) : 1

4 1, 5 (1) : 1

4 2, 5 (1) : 1

4 3, 4 (1) : 1

4 4, 4 (1) : 1

4 5, 3 (1) : 1

4 6, 3 (1) : 1

4 7, 2 (1) : 1

4 8, 2 (1) : 1

5 1, 7 (1) : 1

5 2, 6 (1) : 1

5 3, 5 (1) : 1

5 4, 5 (1) : 1

5 5, 4 (1) : 1

5 6, 4 (1) : 1

5 7, 3 (1) : 1

5 8, 3 (1) : 1

6 1, 8 (1) : 1

6 2, 7 (1) : 1

6 3, 6 (1) : 1

6 4, 6 (1) : 1

6 5, 5 (1) : 1

6 6, 5 (1) : 1

6 7, 4 (1) : 1

6 8, 4 (1) : 1

7 1, 10 (1) : 1

7 2, 9 (1) : 1

7 3, 7 (1) : 1

7 4, 7 (1) : 1

7 5, 6 (1) : 1

7 6, 6 (1) : 1

7 7, 5 (1) : 1

7 8, 4 (1) : 1

8 1, 11 (1) : 1

8 2, 10 (1) : 1

8 3, 9 (1) : 1

8 4, 8 (1) : 1

8 5, 8 (1) : 1

8 6, 7 (1) : 1

8 7, 6 (1) : 1

8 8, 5 (1) : 1

9 1, 12 (1) : 1

9 2, 11 (1) : 1

9 3, 10 (1) : 1

9 4, 9 (1) : 1

9 5, 9 (1) : 1

9 6, 8 (1) : 1

9 7, 7 (1) : 1

9 8, 6 (1) : 1

Appendix B

Parameters of Machines

S No	Induction Machine Parameters	Predefined Values
1.	Stator Resistance(R_s)	2.7+R
2.	Rotor Resistance(R_r)	2.23
3.	Stator Inductance(L_s)	0.3562
4.	Rotor Inductance(L_r)	0.3362
5.	Mutual Inductance(L_m)	0.3425
6.	Friction Coefficient (J)	0.0025
7.	Number of poles (N)	2

Table 4.1 Technical specifications of the induction machine system

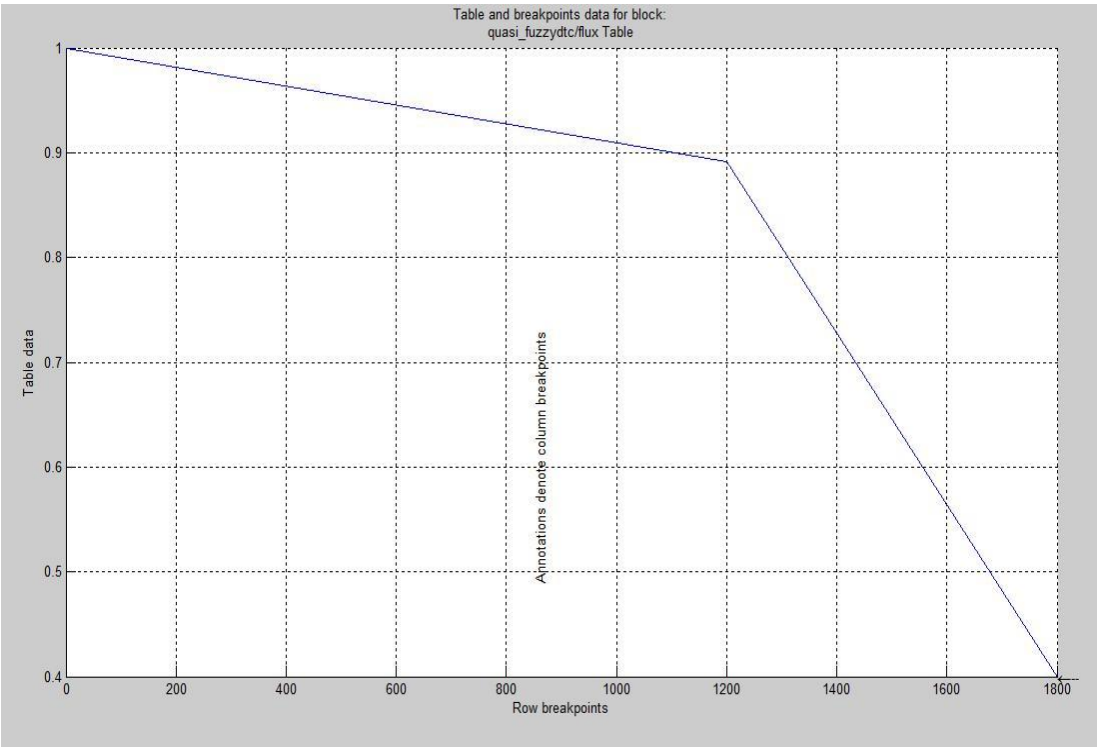

Figure 4.11 Flux table

Appendix C

Hysteresis Controller

The two level hysteresis controller for flux with a total hysteresis band of $2\Delta\psi_s$ (Fig. 4.9) is modeled to output 1 or -1 as per following conditions:

$d\psi = 1$ if $|\psi_s| \leq |\psi_{s\_ref}| - |\Delta\psi_s|$

$d\psi = -1$ if $|\psi_s| \geq |\psi_{s\_ref}| + |\Delta\psi_s|$

The three level hysteresis controller of torque which compares reference torque signal generated by speed regulator with estimated torque is modeled to output 1, 0 or -1 as per following specifications:

$dt_e = 1$ if $|t_e| \leq |t_{e\_ref}| - |\Delta t_e|$

$dt_e = 0$ if $|t_e| \geq t_{e\_ref}$

$dt_e = -1$ if $|t_e| \leq |t_{e\_ref}| + |\Delta t_e|$

$dt_e = 0$ if $|t_e| \leq t_{e\_ref}$

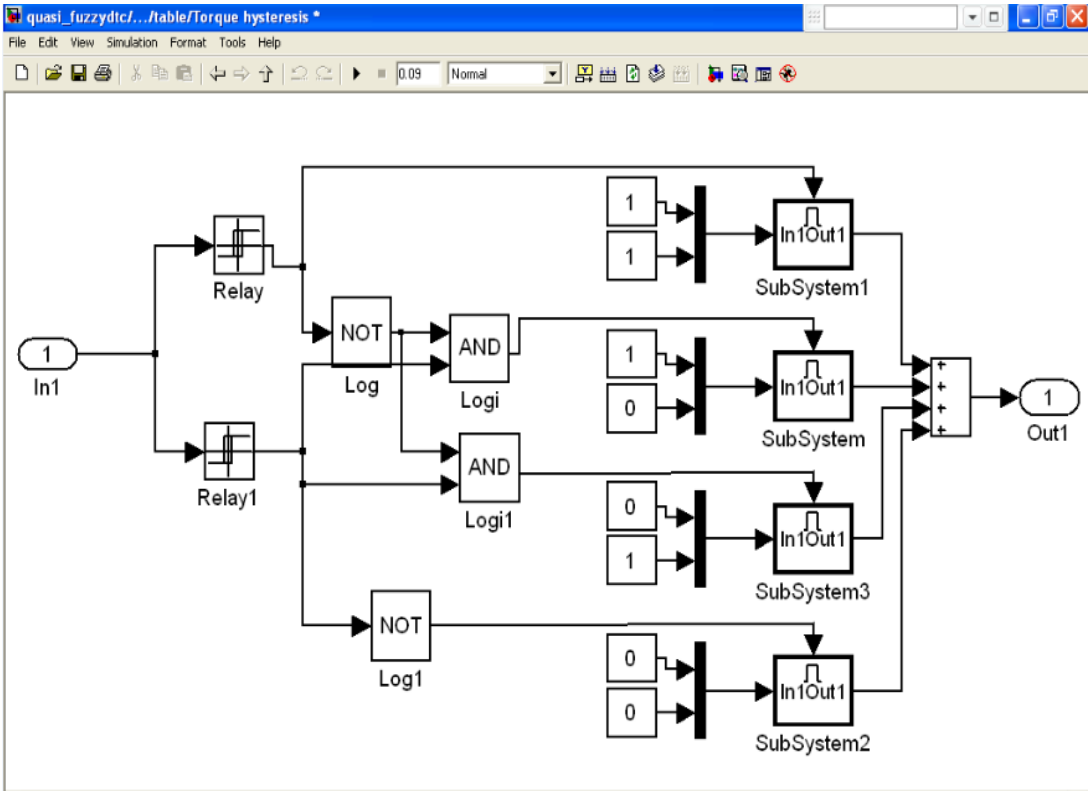

Figure 4.12Hysteresis controller

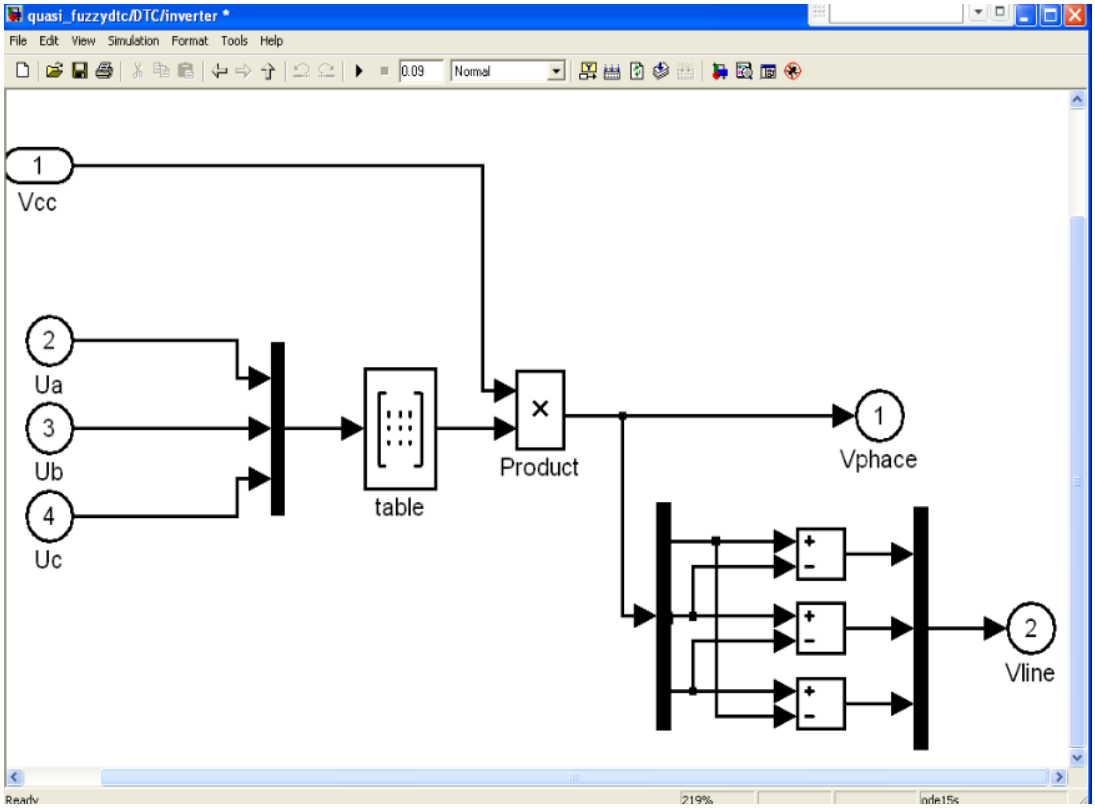

Figure 4.13 Inverter model

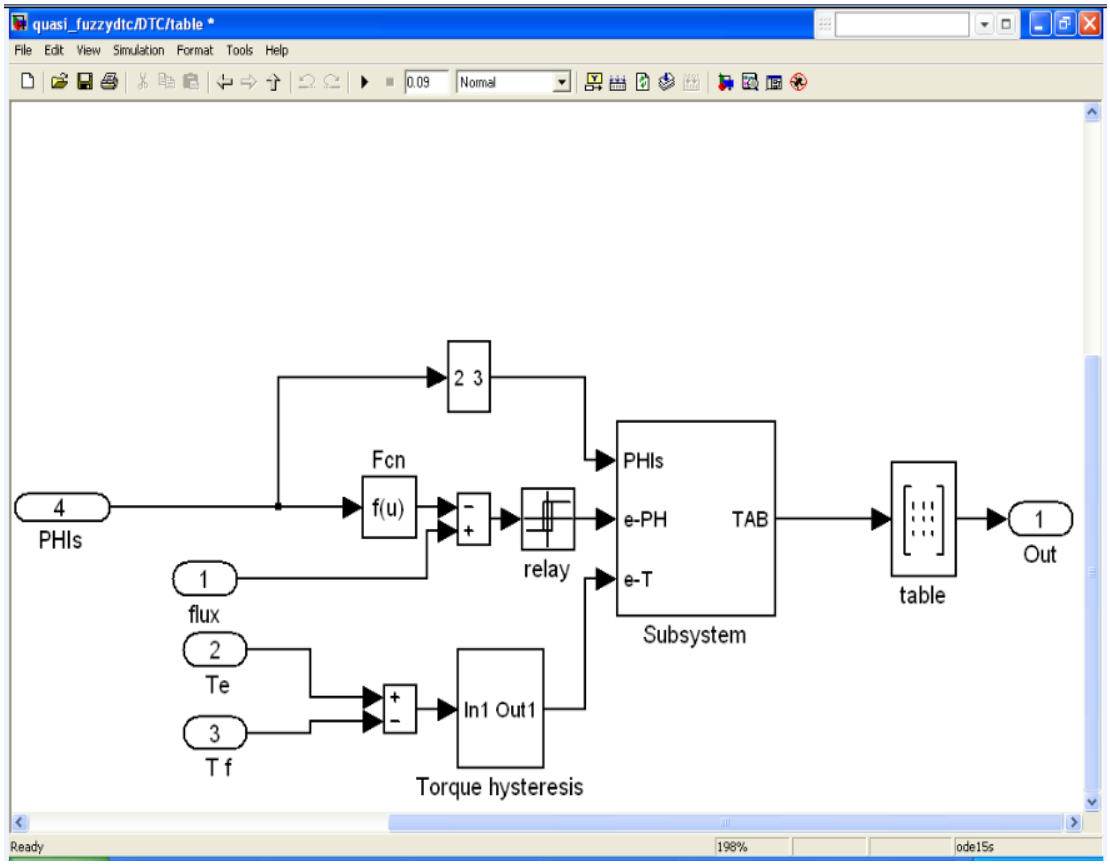

Figure 4.14 DTC table

Appendix D

4.5 Stator flux based field orientation

Initially Rotor flux field orientated induction machine drive systems have been shown to offer high performance as well as independent control on torque and flux made to eliminate flux sensors in an indirect field oriented (IFO) system without sacrificing performance. A commonly used method is to estimate rotor flux from terminal quantities. The accuracy of the estimated stator flux depends on the accuracy of the estimated stator resistance. Usually the stator resistance can be measured with reasonable accuracy and it is relatively easy to adapt to its slow variation with temperature (Bose, 2002).

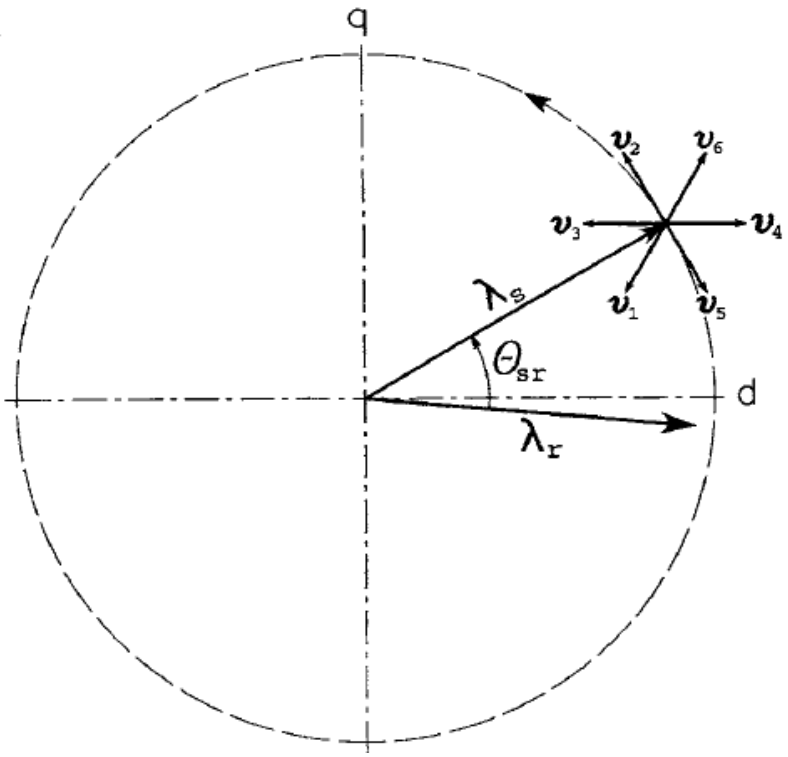

Figure 4.15 Illustration of the principles of control of stator flux and developed torque by inverter state selection (Trzynadlowski, 2001)

	v_K	v_{K+1}	v_{K+2}	v_{K+3}	v_{K+4}	v_{K+5}	v_Z
λ_s	↗↗	↗	↘	↘↘	↘	↗	-
T_M	?	↗	↗	?	↘	↘	↘

Table 4.2 Impact of individual voltage on the stator flux and developed torque (Trzynadlowski, 2001)

The DTC classical look up table is as follows:

Fl_error(ϕ)	Te_error(τ)	S_1	S_2	S_3	S_4	S_5	S_6
FI	T = 1	V_2	V_3	V_4	V_5	V_6	V_1
	T = 0	V_0	V_7	V_0	V_7	V_0	V_7
	T =-1	V_6	V_1	V_2	V_3	V_4	V_5
FD	T= 1	V_3	V_4	V_5	V_6	V_1	V_2
	T= 0	V_7	V_0	V_7	V_0	V_7	V_0
	T =-1	V_5	V_6	Vi	V_2	V_3	V_4

Table 4.3 Look up table for Direct Torque Control (Bose, 2002)

FD/FI: flux decrease/increase. T=-1/0/1: torque decrease/equal/increase.

S_x: stator flux sector.ϕ: stator flux modulus error after the hysteresis block.

τ: torque error after the hysteresis block.